

Electronic Supplementary Information

A Comparative Study on *nido*- and *closو*-Carborane Supported Zinc-salen Catalysts for the ROCOP of Epoxides and Anhydrides

Jin-Bian Xue[†], Jia-Ni Wang[†], Ke-Cheng Chen, Qian Cheng, Jia-Ying Zhang, Xu-Qiong Xiao^{*}

Key Laboratory of Organosilicon Chemistry and Material Technology, Ministry of Education,
Zhejiang Key Laboratory of Organosilicon Material Technology,
College of Material, Chemistry and Chemical Engineering, Hangzhou Normal University,
No. 2318 Yuhangtang Rd. Hangzhou, 311121, Zhejiang (China)

Email: xqxiao@hznu.edu.cn

Table of Contents:

(1) Experimental details	2
(2) NMR Spectra	6
(3) General Procedure for ROCOP	31
(4) GPC data of polymers	34
(5) X-ray crystallographic details	35
(6) References	39

(1) Experimental details

1.1 General remarks

Manipulation of air-sensitive complexes were performed under a controlled dry argon or nitrogen atmosphere using standard Schlenk techniques. Glassware was stored in an oven at 150°C for at least 4 hours and evacuated before use. The monomers (cyclohexane oxide, epichlorohydrin, 4-vinyl cyclohexene oxide, 1,2-epoxyhexane) were dried by refluxing over CaH₂ for 3 days and distilled under nitrogen atmosphere prior to use. All other reagents and solvents (ZnCl₂, ZnEt₂, Zn(OAc)₂, phthalic anhydride) were commercially available and used without further purification. Compounds **1** were prepared using literature procedures. ¹ ¹H and ¹³C{¹H} NMR spectra were recorded on Bruker Avance-400 or Avance-500 spectrometers. The two-dimensional HMBC and ¹¹B{¹H} NMR spectra were measured with an Avance-500 instrument. ¹H and ¹³C{¹H} NMR spectra were calibrated against the residual signal of the solvent as internal references. The ¹¹B{¹H} NMR were calibrated against external standards (δ ¹¹B(BF₃·Et₂O) = 0.00). High-resolution mass spectra were measured with a Bruker Daltonics Autoflex II TM MALDI-TOF spectrometer. Gel Permeation Chromatography (GPC) analysis was performed using tetrahydrofuran as eluent (flow rate: 1 mL/min, at 40 °C) on a PL 50 apparatus, with molecular weights and molecular weight distributions reported relative to polystyrene standards.

1.2 The synthesis of complexes **2a-2d**

A mixture of **1** (0.20 mmol) and Zn(OAC)₂ (55 mg, 0.30 mmol) was stirred in ethanol at room temperature for 24 hours. The reaction mixture gradually changed from turbid to clear and transparent. The resulting solution was then concentrated until microcrystals began to form. Upon the addition of n-hexane, a yellow solid (**2a-2d**) was obtained.

2a. Yield: 109 mg, 83%. **¹H NMR** (400.13 MHz, Acetone-*d*₆): δ 8.59 (s, 4H, N=CH), 7.60 (d, *J* = 8 Hz, 4H, *H*_{Ph}), 7.25 (t, *J* = 8.0 Hz, 4H, *H*_{Ph}), 7.05-6.90 (m, 8H, *H*_{Ph}), -2.19 (s, 2H, B-H-B); **¹³C{¹H} NMR** (100.61 MHz, Acetone-*d*₆): δ 163.34 (N=CH), 162.37 (C_{Ph}), 135.59 (C_{Ph}), 133.47 (C_{Ph}), 122.04 (C_{Ph}), 121.07 (C_{Ph}), 118.16 (C_{Ph}), 78.02 (C_o-carb); **¹¹B{¹H} NMR** (160.46

MHz, Acetone-*d*₆): δ -11.78, -19.53, -22.47,-34.50,-37.07. HRMS (ESI): m/z calcd. For [C₁₆H₁₉O₂N₂B₉Zn]⁻: 434.1732; found: [2a-Zn(H₂O)₂]²⁻: 434.1709.

2b. Yield: 123 mg, 80%. **¹H NMR** (400.13 MHz, Acetone-*d*₆): δ 8.52 (s, 4H, N=CH), 7.66-6.87 (m, 12H, H_{Ph}), 1.51 (s, 36H, *t*Bu), -2.29 (s, 2H, B-H-B); **¹³C{¹H} NMR** (100.62 MHz, Acetone-*d*₆): δ 163.09 (N=CH), 161.92 (C_{Ph}), 143.03 (C_{Ph}), 133.82 (C_{Ph}), 131.03 (C_{Ph}), 123.18 (C_{Ph}), 119.18 (C_{Ph}), 78.41 (C_o-carb), 35.65 (CMe₃), 30.11 (CMe₃); **¹¹B{¹H} NMR** (160.46 MHz, Acetone-*d*₆): δ -9.67, -20.40, -32.28, -34.84; HRMS (ESI): m/z calcd. for [C₂₄H₃₅O₂N₂B₉Zn]⁻: 547.3045; found: [2b-Zn(H₂O)₂]²⁻: 547.3013.

2c. Yield: 144 mg, 82%. **¹H NMR** (400.13 MHz, Acetone-*d*₆): δ 8.56 (s, 4H, N=CH), 7.54 (d, 4H, H_{Ph}), 7.46 (d, 4H, H_{Ph}), 1.52 (s, 36H, *t*Bu), 1.35 (s, 36H, *t*Bu), -2.29 (s, 2H, B-H-B); **¹³C{¹H} NMR** (100.61 MHz, Acetone-*d*₆): δ 163.80 (N=CH), 159.24 (C_{Ph}), 142.54 (C_{Ph}), 141.88 (C_{Ph}), 130.43 (C_{Ph}), 128.95 (C_{Ph}), 122.72 (C_{Ph}), 78.61 (C_o-carb), 36.07 (CMe₃), 34.74 (CMe₃), 31.55 (CMe₃), 30.39 (CMe₃); **¹¹B{¹H} NMR** (160.46 MHz, Acetone-*d*₆): δ -11.28, -21.79, -33.97, -36.28. HRMS (ESI): m/z calcd. for [C₃₂H₅₁O₂N₂B₉Zn]⁻: 658.4194; found [2c-Zn(H₂O)₂]²⁻: 658.4173.

2d. Yield: 154 mg, 90%. **¹H NMR** (400.13 MHz, Acetone-*d*₆): δ 8.50 (s, 4H, N=CH), 8.21 (d, 4H, H_{Ph}), 8.06 (d, 4H, H_{Ph}), 1.48 (s, 36H, *t*Bu), -2.25 (s, 2H, B-H-B); **¹³C{¹H} NMR** (100.61 MHz, Acetone-*d*₆): δ 176.35 (N=CH), 162.15 (C_{Ph}), 143.14 (C_{Ph}), 134.64 (C_{Ph}), 131.53 (C_{Ph}), 124.39 (C_{Ph}), 119.39 (C_{Ph}), 78.68 (C_o-carb), 36.00 (CMe₃), 29.69 (CMe₃); **¹¹B{¹H} NMR** (160.46 MHz, Acetone-*d*₆): δ -14.95, -25.75, -37.82, -40.09. HRMS (ESI): m/z calcd. for [C₃₂H₄₉O₆N₄B₉Zn]⁻: 748.3786; found [2d-Zn(H₂O)₂]²⁻: 748.3765.

1.3 The synthesis of 3a-3d

To a THF (5 mL) solution of **1** (0.20 mmol) and ZnCl₂ (27 mg, 0.20 mmol), Et₃N (0.40 mmol) was slowly added at room temperature. The solution gradually changed from clear to turbid. After stirring for 12 hours, the mixture was filtered, and the filtrate was concentrated under reduced pressure until microcrystals began to form. Upon addition of *n*-hexane, a bright yellow solid (**3**) was obtained.

3a. Yield: 99 mg, 96%. **¹H NMR** (400.13 MHz, Acetone-*d*₆): δ 8.33 (s, 2H, N=CH), 7.38 (d, *J* = 7.6 Hz, 2H, H_{Ph}), 7.25 (t, 2H, H_{Ph}), 7.06(d, *J* = 8 Hz, 2H, H_{Ph}), 6.75 (t, 2H, H_{Ph}), 3.20 (18H,

Et), 1.26 (24H, Et); **¹³C{¹H} NMR** (100.61 MHz, Acetone-*d*₆): δ 165.52 (N=CH), 161.10 (C_{Ph}), 135.75 (C_{Ph}), 133.51 (C_{Ph}), 122.52 (C_{Ph}), 122.15 (C_{Ph}), 117.55 (C_{Ph}), 77.99 (C_o-carb, from HMBC), 47.41 (Et), 9.40 (Et); **¹¹B{¹H} NMR** (160.46MHz, Acetone-*d*₆): δ -9.56, -20.31, -32.19, -34.77; HRMS (ESI): m/z calcd. for [C₁₆H₁₉O₂N₂B₉Zn]⁺: 434.1732; found [3a]⁺: 434.1712.

3b. Yield: 116 mg, 92%. **¹H NMR** (400.13 MHz, Acetone-*d*₆): δ 8.33 (s, 2H, N=CH), 7.14 (d, *J* = 5.5 Hz, 2H, H_{Ph}), 6.99 (d, *J* = 5.9 Hz, 2H, H_{Ph}), 6.36 (t, 2H, H_{Ph}), 2.93 (18H, Et), 1.48 (s, 18H, *t*Bu), 1.14 (24H, Et); **¹³C{¹H} NMR** (100.61 MHz, Acetone-*d*₆): δ 171.77 (N=CH), 162.73 (C_{Ph}), 142.10 (C_{Ph}), 133.80 (C_{Ph}), 129.38 (C_{Ph}), 120.88 (C_{Ph}), 112.19 (C_{Ph}), 78.98, 79.24 (C_o-carb, from HMBC), 47.39 (Et), 35.92 (CM_e₃), 30.14 (CM_e₃), 9.34 (Et); **¹¹B{¹H} NMR** (160.46MHz, Acetone-*d*₆): δ -10.22, -20.59, -32.56, -35.15; HRMS (ESI): m/z calcd. For [C₂₄H₃₅O₂N₂B₉Zn]⁺: 546.2942; found [3b]⁺: 546.2965.

3c. Yield: 136 mg, 92%. **¹H NMR** (400.13 MHz, Acetone-*d*₆): δ 8.36 (s, 2H, N=CH), 7.28 (s, 2H, H_{Ph}), 6.97 (s, 2H, H_{Ph}), 3.00 (18H, Et), 1.50 (s, 18H, *t*Bu), 1.30 (s, 18H, *t*Bu), 1.18 (t, 24H, Et); **¹³C{¹H} NMR** (100.61 MHz, Acetone-*d*₆): δ 169.83 (N=CH), 163.07 (C_{Ph}), 141.40 (C_{Ph}), 133.53 (C_{Ph}), 129.22 (C_{Ph}), 127.42 (C_{Ph}), 119.60 (C_{Ph}), 79.76 (C_o-carb, from HMBC), 47.43 (Et₃N), 36.19 (CM_e₃), 34.29 (CM_e₃), 31.97 (CM_e₃), 9.47 (Et); **¹¹B{¹H} NMR** (160.46MHz, Acetone-*d*₆): δ -10.16, -12.01, -20.44, -32.51, -34.95; HRMS(ESI): m/z calcd. for [C₃₂H₅₁O₂N₂B₉Zn]⁺: 658.4236; found [3c]⁺: 658.4220.

3d. Yield: 135 mg, 94%. **¹H NMR** (400.13 MHz, Acetone-*d*₆): δ 8.38 (s, 2H, N=CH), 8.14 (s, 2H, H_{Ph}), 8.02 (s, 2H, H_{Ph}), 3.08 (s, 24H, Et), 1.49 (s, 18H, *t*Bu), 1.23 (t, 36H, Et); **¹³C{¹H} NMR** (100.61 MHz, Acetone-*d*₆): δ 177.05 (N=CH), 161.25 (C_{Ph}), 143.21 (C_{Ph}), 134.02 (C_{Ph}), 131.58 (C_{Ph}), 124.18 (C_{Ph}), 120.04 (C_{Ph}), 78.50 (C_o-carb, from HMBC), 47.50 (Et₃N), 36.21 (CM_e₃), 9.21 (Et₃N); **¹¹B{¹H} NMR** (160.46MHz, Acetone-*d*₆): δ -10.42, -20.55, -32.51, -35.08; HRMS(ESI): m/z calcd. for [C₂₄H₃₃O₆N₄B₉Zn]⁺: 636.2685; found [3d]⁺: 636.2670.

1.4 The synthesis of 4a-4d

To a THF (5 mL) solution of **1** (0.20 mmol) and ZnCl₂ (27 mg, 0.20 mmol), Et₃N (1.20 mmol) was slowly added at room temperature. The solution gradually changed from clear to turbid. After stirring for 7 hours, the mixture was filtered, and the filtrate was concentrated

under reduced pressure to afford the crude product, which was further purified by column chromatography (DCM:Hexane=10:1).

4a. Yield: 41 mg, 40%. **¹H NMR** (400.13 MHz, Acetone-*d*₆): δ 8.34 (s, 2H, N=CH), 7.40 (d, *J* = 7.7 Hz, 2H, *H*_{Ph}), 7.27(t, 2H, *H*_{Ph}), 7.13(m, 2H, *H*_{Ph}), 6.77 (m, 2H, *H*_{Ph}); **¹³C{¹H} NMR** (100.61 MHz, Acetone-*d*₆): δ 164.11 (N=CH), 163.11 (*C*_{Ph}), 136.29 (*C*_{Ph}), 134.16 (*C*_{Ph}), 122.73 (*C*_{Ph}), 121.73 (*C*_{Ph}), 118.72 (*C*_{Ph}), 91.42 (*C*_{o-carb}, from HMBC); **¹¹B{¹H} NMR** (160.46MHz, Acetone-*d*₆): δ -9.58, -15.68; HRMS (ESI): m/z calcd. for [C₁₆H₂₁O₂N₂B₁₀ZnNa]⁺: 470.2556; found [4a+Na]⁺: 470.2566.

4b. Yield: 56 mg, 44%. **¹H NMR** (400.13 MHz, Acetone-*d*₆): δ 8.67 (s, 2H, N=CH), 7.34 (d, *J* = 8 Hz, 2H, *H*_{Ph}), 7.18 (d, *J* = 8 Hz, 2H, *H*_{Ph}), 6.46 (t, *J* = 8 Hz, 2H, *H*_{Ph}), 1.48 (s, 18H, *tBu*); **¹³C{¹H} NMR** (100.61 MHz, Acetone-*d*₆): δ 169.91 (N=CH), 162.96 (*C*_{Ph}), 142.88 (*C*_{Ph}), 133.80 (*C*_{Ph}), 133.68 (*C*_{Ph}), 130.83(*C*_{Ph}), 130.74 (*C*_{Ph}), 122.90 (*C*_{Ph}), 89.72 (*C*_{o-carb}, from HMBC), 35.60 (CMe₃); **¹¹B{¹H} NMR** (160.46MHz, Acetone-*d*₆): δ -8.56, -12.5; HRMS (ESI): m/z calcd. for [C₂₄H₃₈O₂N₂B₁₀Zn]⁺: 560.3155; found [4b+H]⁺: 560.3259.

4c. Yield: 77 mg, 52%. **¹H NMR** (400.13 MHz, Acetone-*d*₆): δ 8.33 (s, 2H, N=CH), 7.26 (s, 2H, *H*_{Ph}), 6.95 (s, 2H, *H*_{Ph}), 1.49 (s, 18H, *tBu*), 1.29 (s, 18H, *tBu*); **¹³C{¹H} NMR** (100.61 MHz, Acetone-*d*₆): δ 163.71 (N=CH), 142.40 (*C*_{Ph}), 132.41 (*C*_{Ph}), 130.20(*C*_{Ph}), 129.42 (*C*_{Ph}), 128.61 (*C*_{Ph}), 90.74 (*C*_{o-carb}, from HMBC), 36.20 (CMe₃), 34.72 (CMe₃), 31.76 (CMe₃), 30.49 (CMe₃); **¹¹B {¹H} NMR** (160.46MHz, Acetone-*d*₆): δ -7.2, -12.11,-14.24.

4d. Yield: 59 mg, 41%. **¹H NMR** (400.13 MHz, Acetone-*d*₆): δ 8.40 (s, 2H, N=CH), 8.15 (s, 2H, *H*_{Ph}), 8.02 (s, 2H, *H*_{Ph}), 1.49 (s, 18H, *tBu*); **¹³C{¹H} NMR** (100.61 MHz, Acetone-*d*₆): δ 176.49 (N=CH), 162.22 (*C*_{Ph}), 143.20 (*C*_{Ph}), 134.67 (*C*_{Ph}), 131.62 (*C*_{Ph}), 124.41 (*C*_{Ph}), 119.53 (*C*_{Ph}), 92.34(*C*_{o-carb}, from HMBC), 36.10 (CMe₃); **¹¹B{¹H} NMR** (160.46MHz, Acetone-*d*₆): δ -7.22, -12.25.

1.5 The synthesis of 1b and 1d

A flask equipped with Dean-Stark distillation apparatus was added toluene (20 mL), the corresponding aldehyde (11.5 mmol), compound **1** (1.00 g, 5.75 mmol) and a few drops of trifluoroacetic acid. After the mixture was refluxed for 6 hours, all the volatiles were removed under reduced pressure to give a slightly orange crude product, which was

recrystallized in ethanol to afford **1** as yellow solid.

1b. Yield: 1.842 g, 65%. **¹H NMR** (400.13 MHz, CDCl₃): δ 11.77 (s, 2H, OH), 8.72 (s, 2H, N=CH), 7.46 (d, 2H, H_{Ph}), 7.28 (d, 2H, H_{Ph}), 6.92 (t, 2H, H_{Ph}), 1.39 (s, 18H, tBu); **¹³C{¹H} NMR** (100.61 MHz, CDCl₃): δ 171.41 (N=CH), 160.74 (C_{Ph}), 138.31 (C_{Ph}), 132.76 (C_{Ph}), 132.23 (C_{Ph}), 119.19 (C_{Ph}), 117.87 (C_{Ph}), 93.81 (C_{cage}), 35.12 (CMe₃), 29.44 (CMe₃); **¹¹B{¹H} NMR** (160.46 MHz, CDCl₃): δ -7.49, -9.43, -12.30. HRMS(ESI): m/z calcd. for [C₂₄H₃₈O₂N₂B₉]⁻: 484.3829; found: [1b]⁻: 484.3818.

1d. Yield: 1.996 g, 61%. **¹H NMR** (400.13 MHz, CDCl₃): δ 12.56 (s, 2H, OH), 8.86 (s, 2H, N=CH), 8.34 (s, 4H, H_{Ph}), 1.41 (s, 18H, tBu); **¹³C{¹H} NMR** (100.61 MHz, CDCl₃): δ 170.75 (N=CH), 165.35 (C_{Ph}), 140.37 (C_{Ph}), 140.06 (C_{Ph}), 128.28 (C_{Ph}), 127.49 (C_{Ph}), 116.97 (C_{Ph}), 92.28 (C_{cage}), 35.60 (CMe₃), 29.07 (CMe₃); **¹¹B{¹H} NMR** (160.46 MHz, CDCl₃): δ -7.80, -12.35. HRMS (ESI): m/z calcd. for [C₂₄H₃₆O₆N₄B₉]⁻: 574.3509, found [1d]⁻: 574.3520.

(2) NMR Spectra

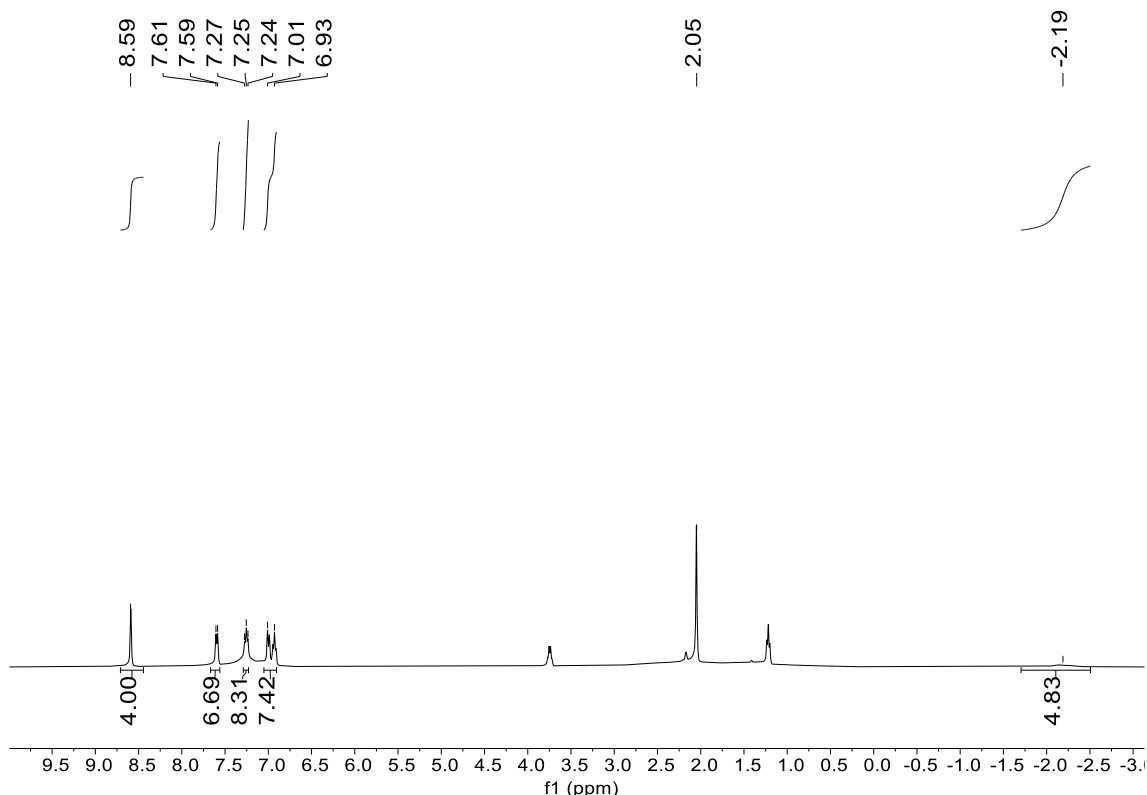


Figure S1. **¹H NMR** (Acetone-d₆, 400.13 MHz) spectrum of compound **2a**.

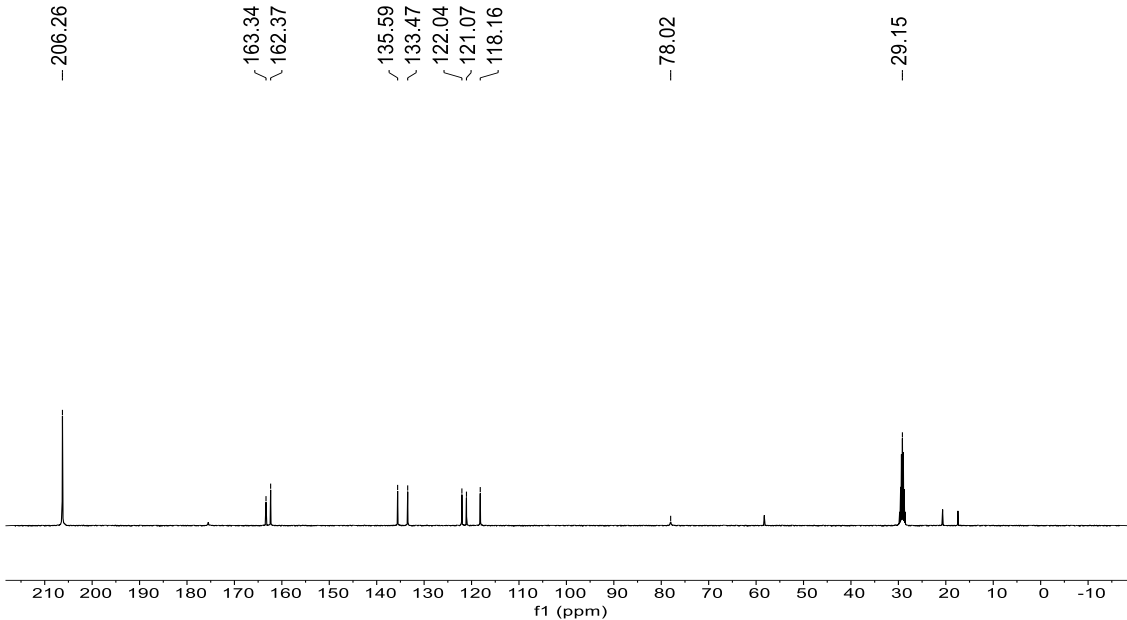


Figure S2. $^{13}\text{C}\{\text{H}\}$ NMR (Acetone- d_6 , 100.62 MHz) spectrum of compound **2a**.

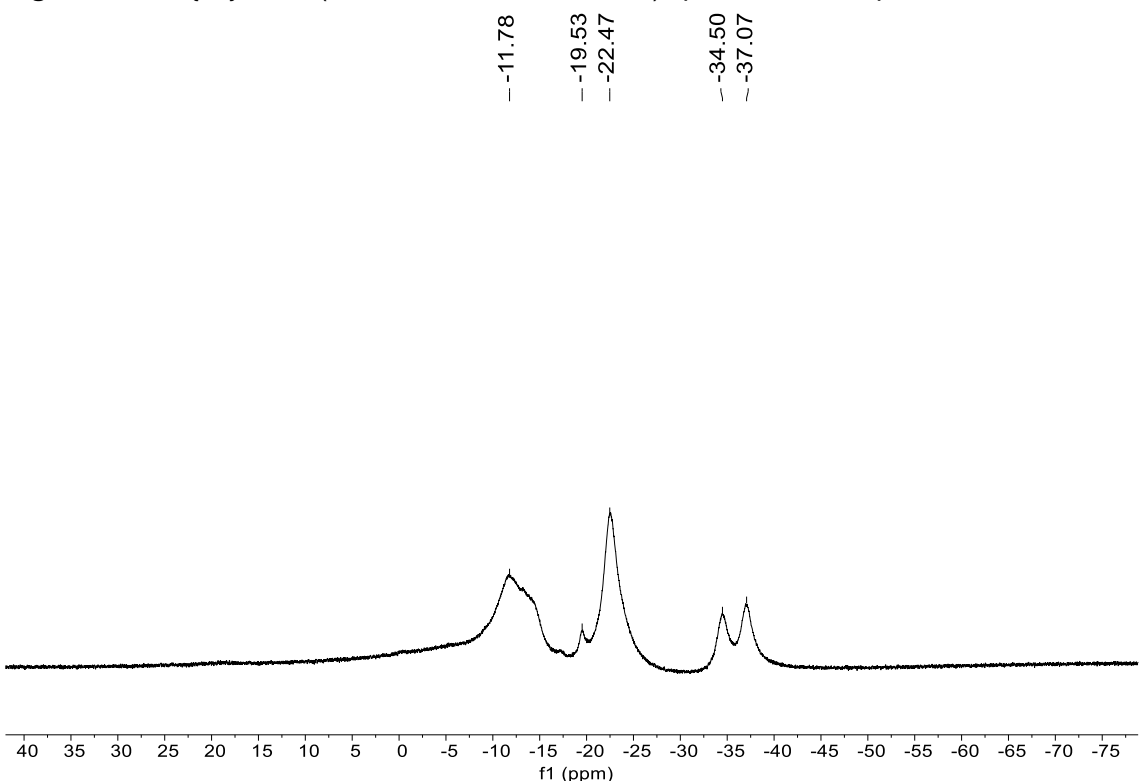


Figure S3. $^{11}\text{B}\{\text{H}\}$ NMR (Acetone- d_6 , 160.46 MHz) spectrum of compound **2a**.

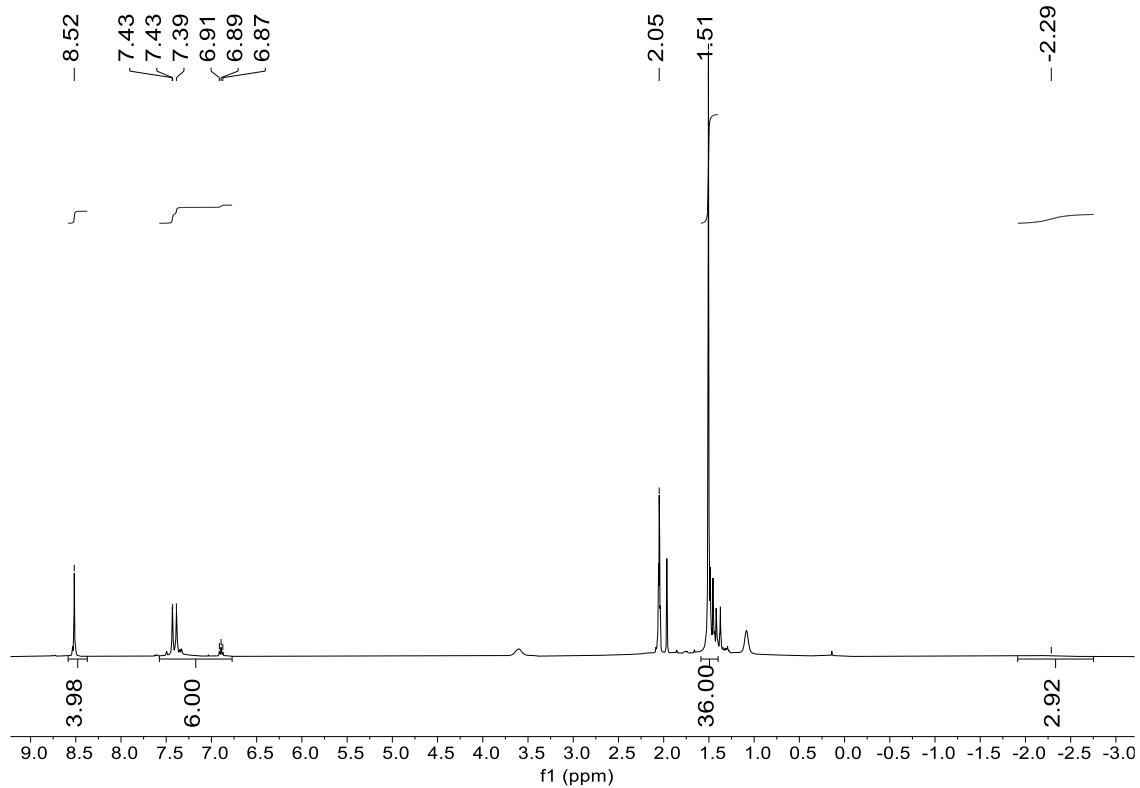


Figure S4. ¹H NMR (Acetone-*d*₆, 400.13 MHz) spectrum of compound **2b**.

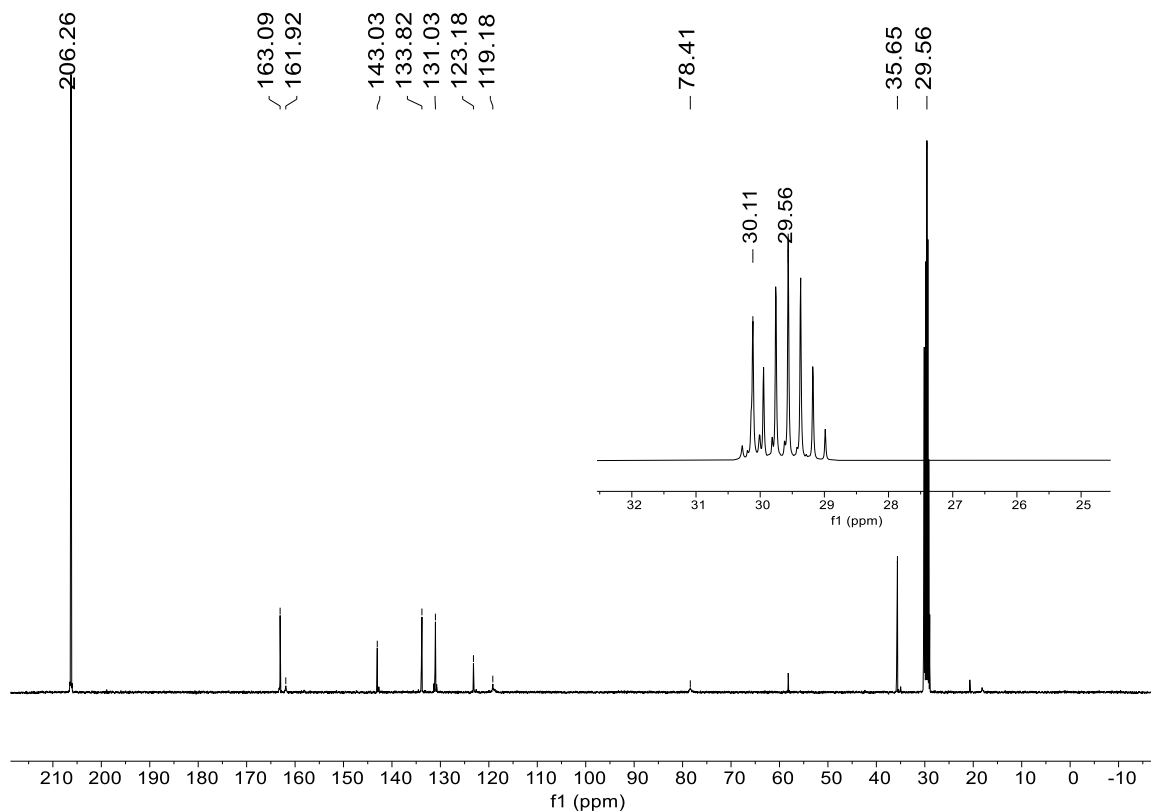


Figure S5. ¹³C{¹H} NMR (Acetone-*d*₆, 100.62 MHz) spectrum of compound **2b**.

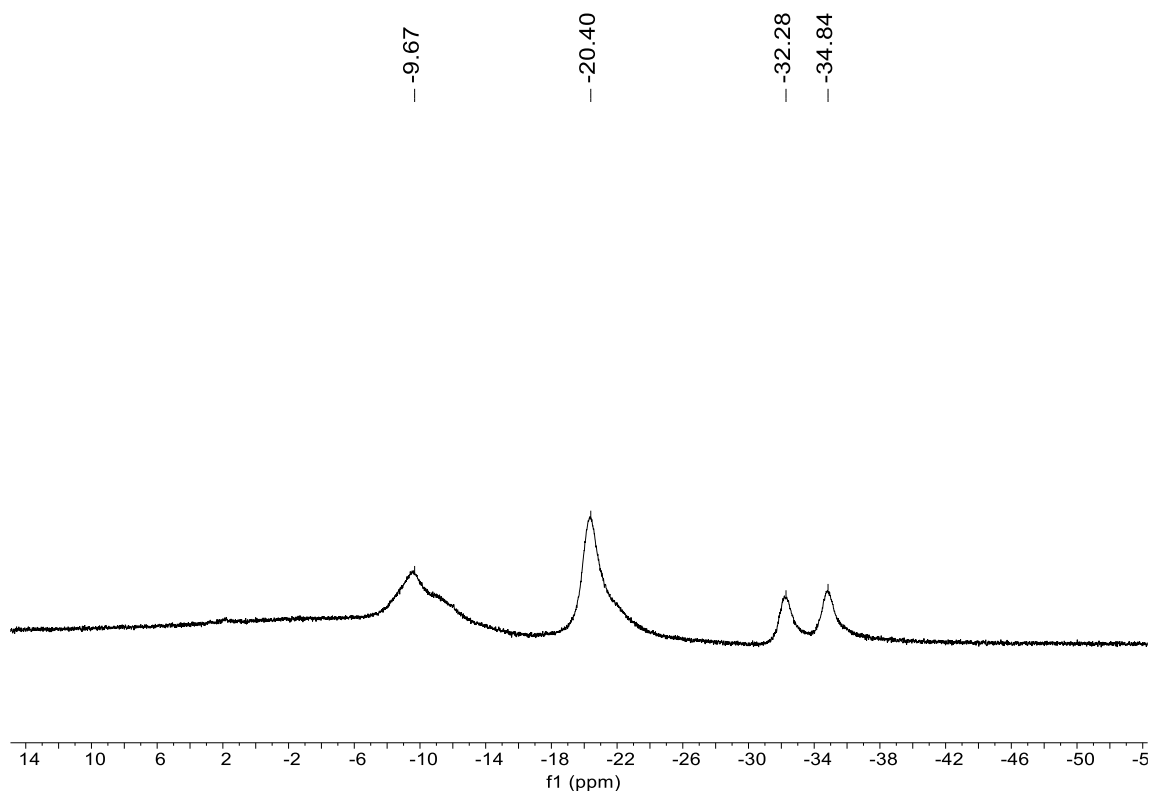


Figure S6. ¹¹B{¹H} NMR (Acetone-*d*₆, 160.46 MHz) spectrum of compound **2b**.

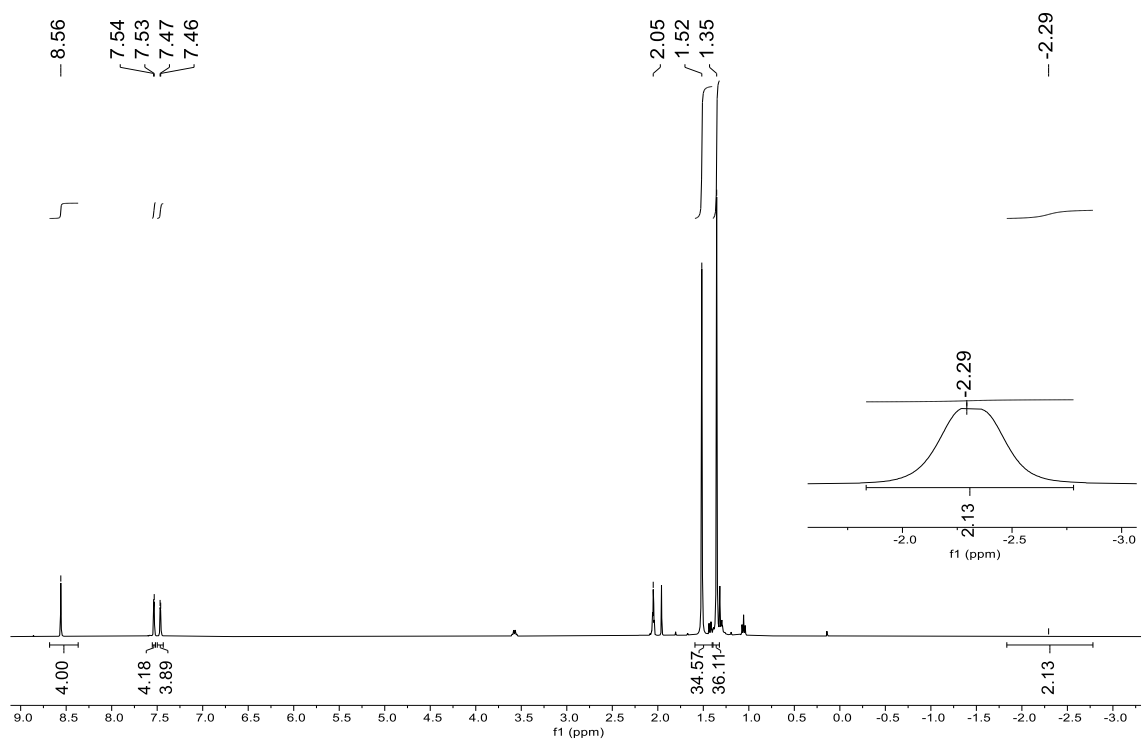


Figure S7. ¹H NMR (Acetone-*d*₆, 400.13 MHz) spectrum of compound **2c**.

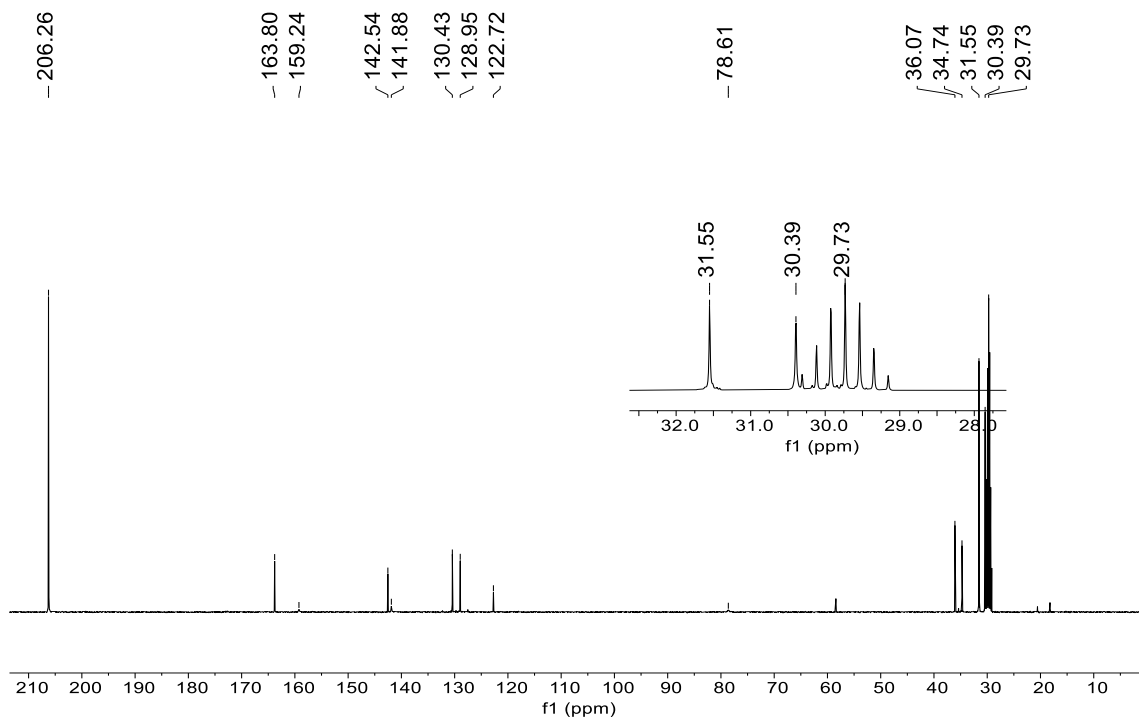


Figure S8. $^{13}\text{C}\{\text{H}\}$ NMR (Acetone- d_6 , 100.62 MHz) spectrum of compound **2c**.

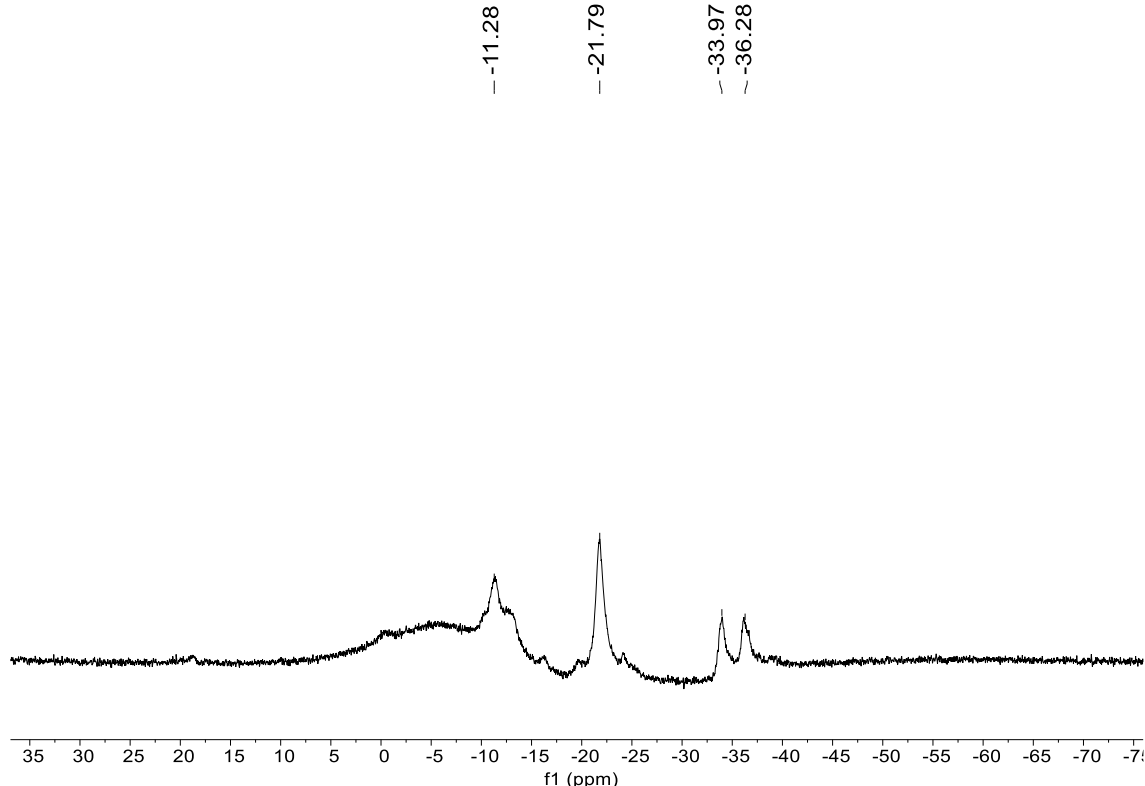


Figure S9. $^{11}\text{B}\{\text{H}\}$ NMR (Acetone- d_6 , 160.46 MHz) spectrum of compound **2c**

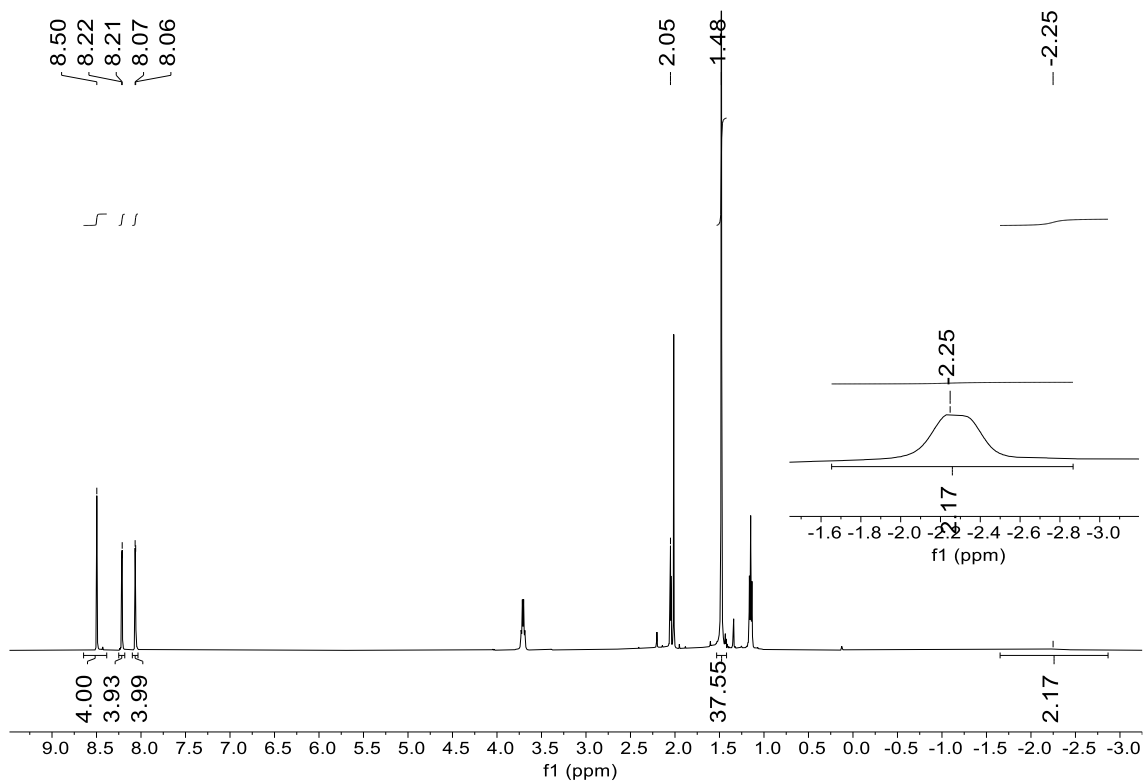


Figure S10 ^1H NMR (Acetone- d_6 , 400.13 MHz) spectrum of compound **2d**.

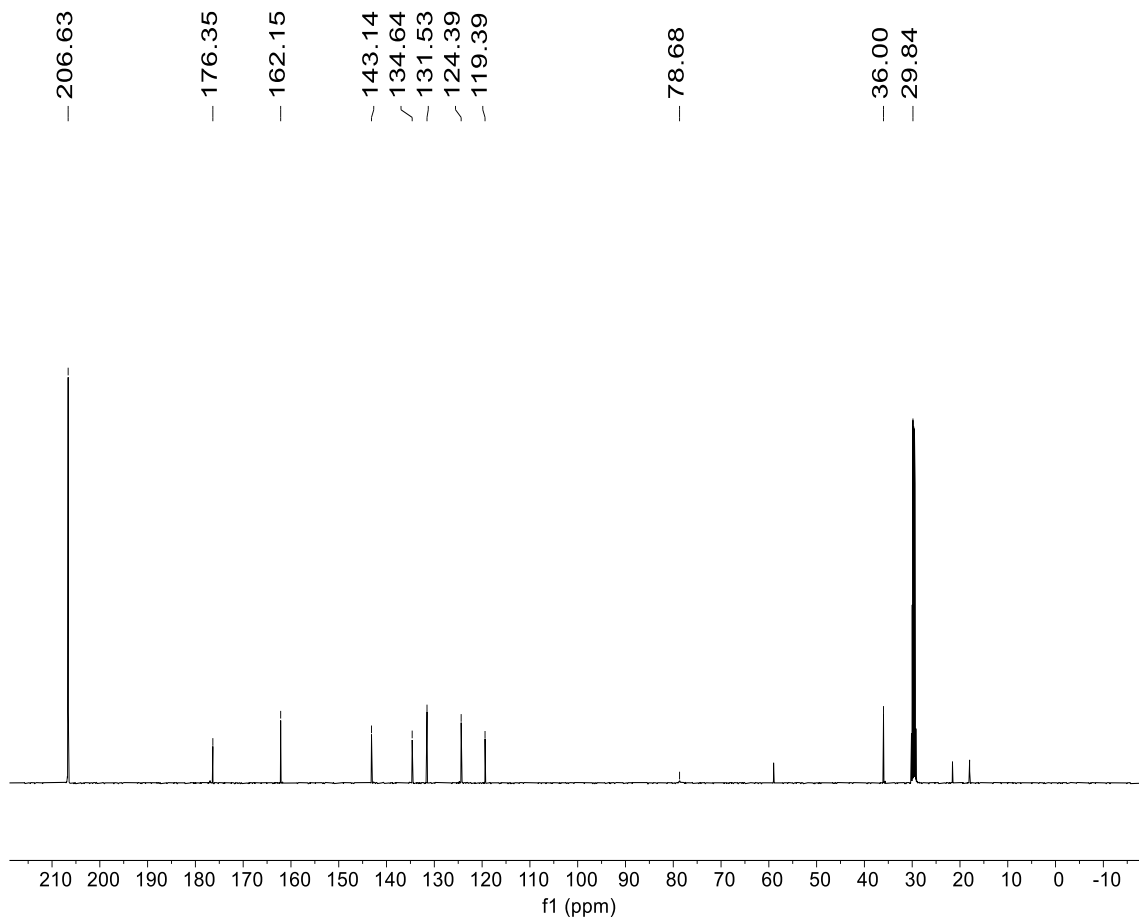


Figure S11. $^{13}\text{C}\{^1\text{H}\}$ NMR (Acetone- d_6 , 100.62 MHz) spectrum of compound **2d**.

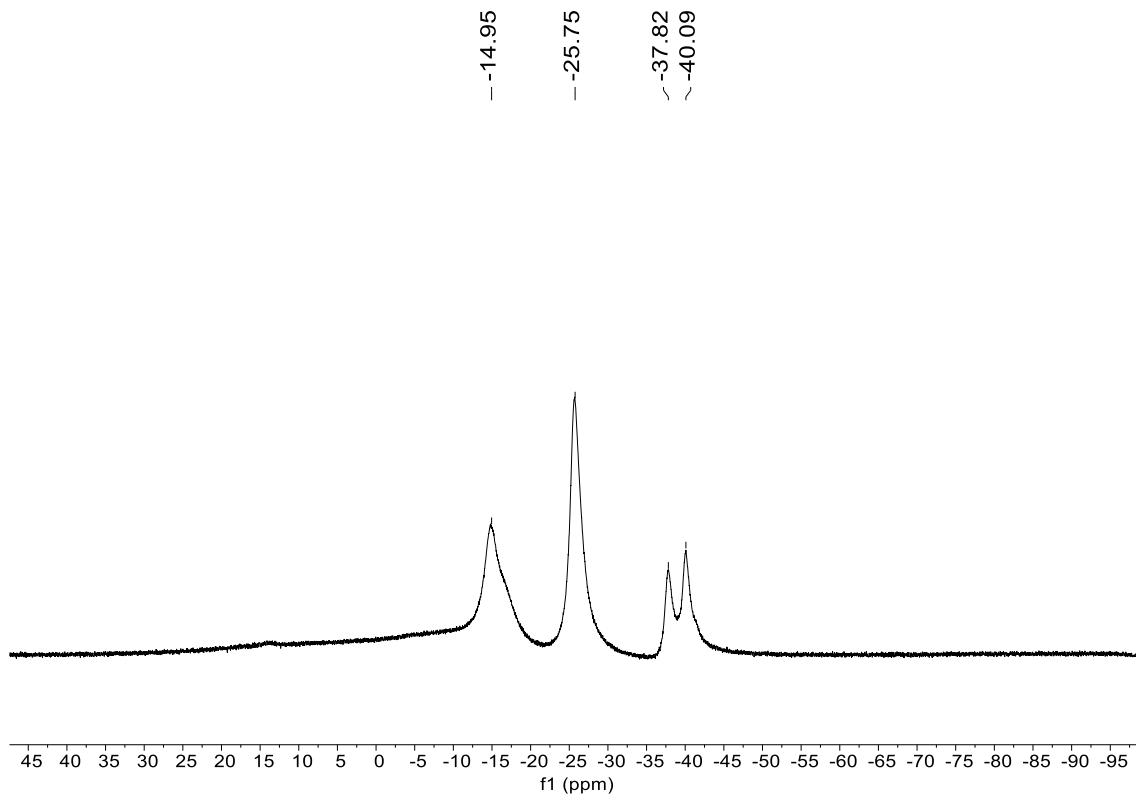


Figure S12. $^{11}\text{B}\{\text{H}\}$ NMR (Acetone- d_6 , 160.46 MHz) spectrum of compound **2d**.

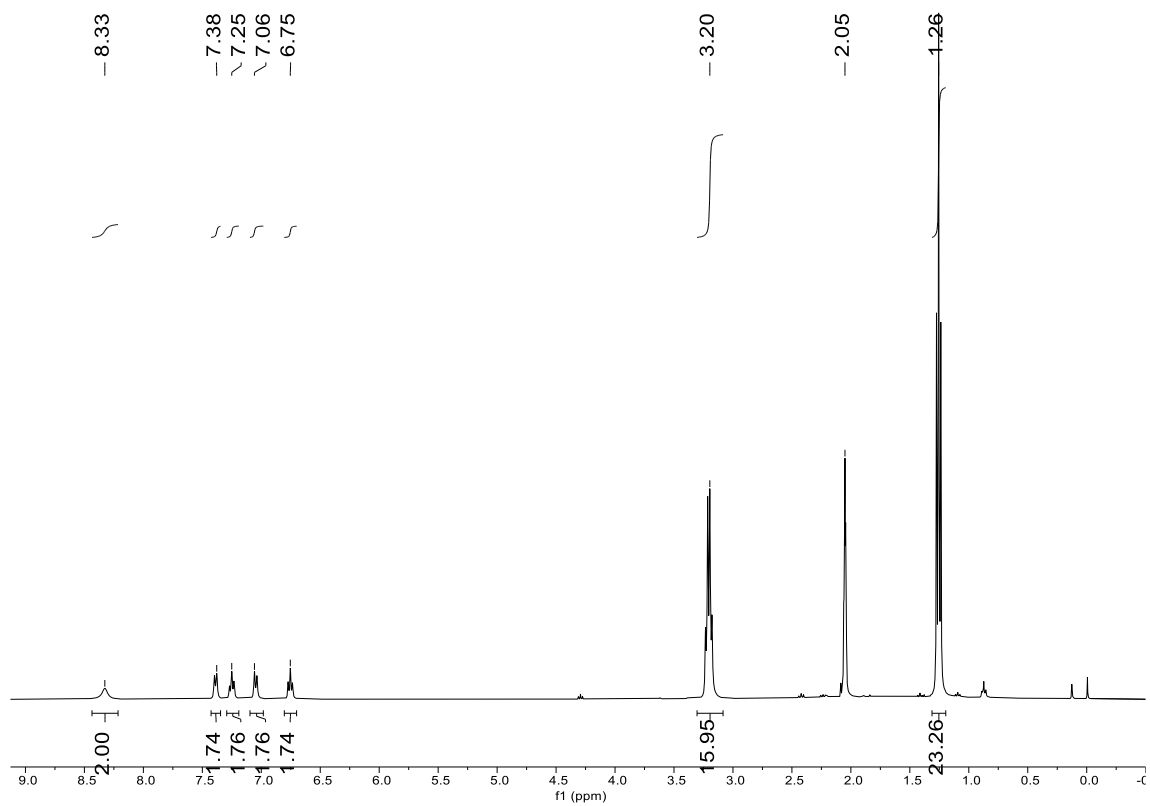


Figure S13. ^1H NMR (Acetone- d_6 , 400.13 MHz) spectrum of compound **3a**.

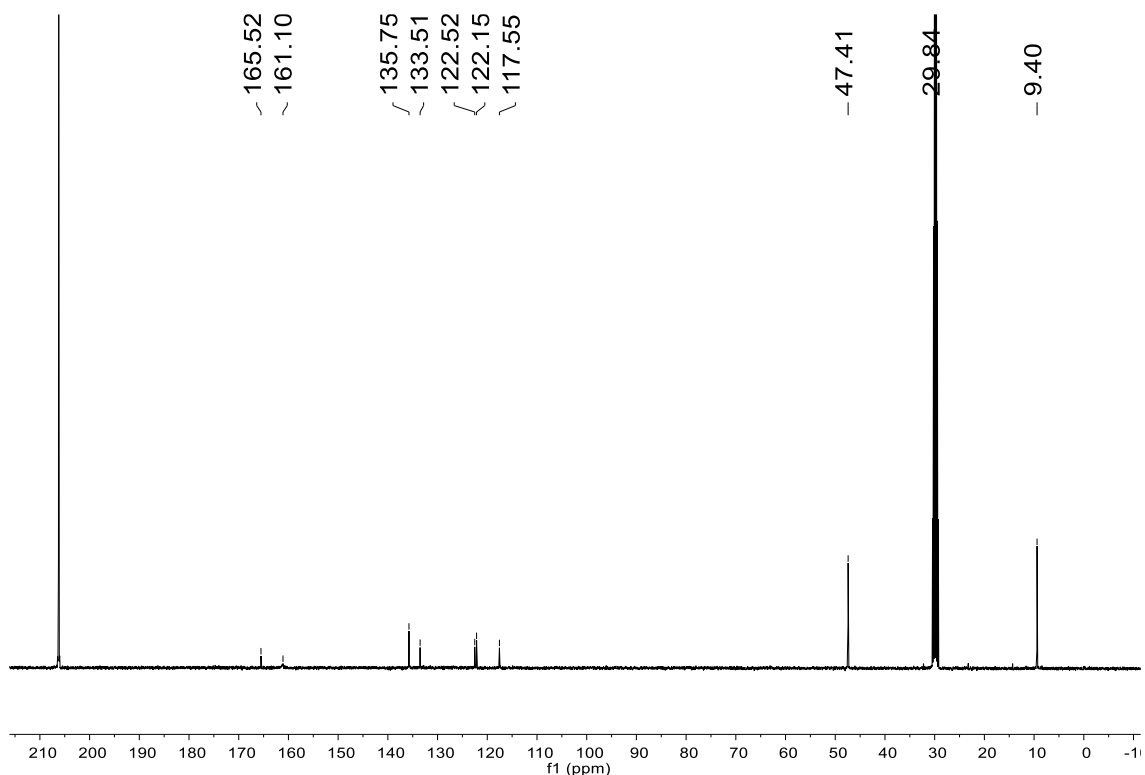


Figure S14. ¹³C{¹H} NMR (Acetone-*d*₆, 100.62 MHz) spectrum of compound 3a.

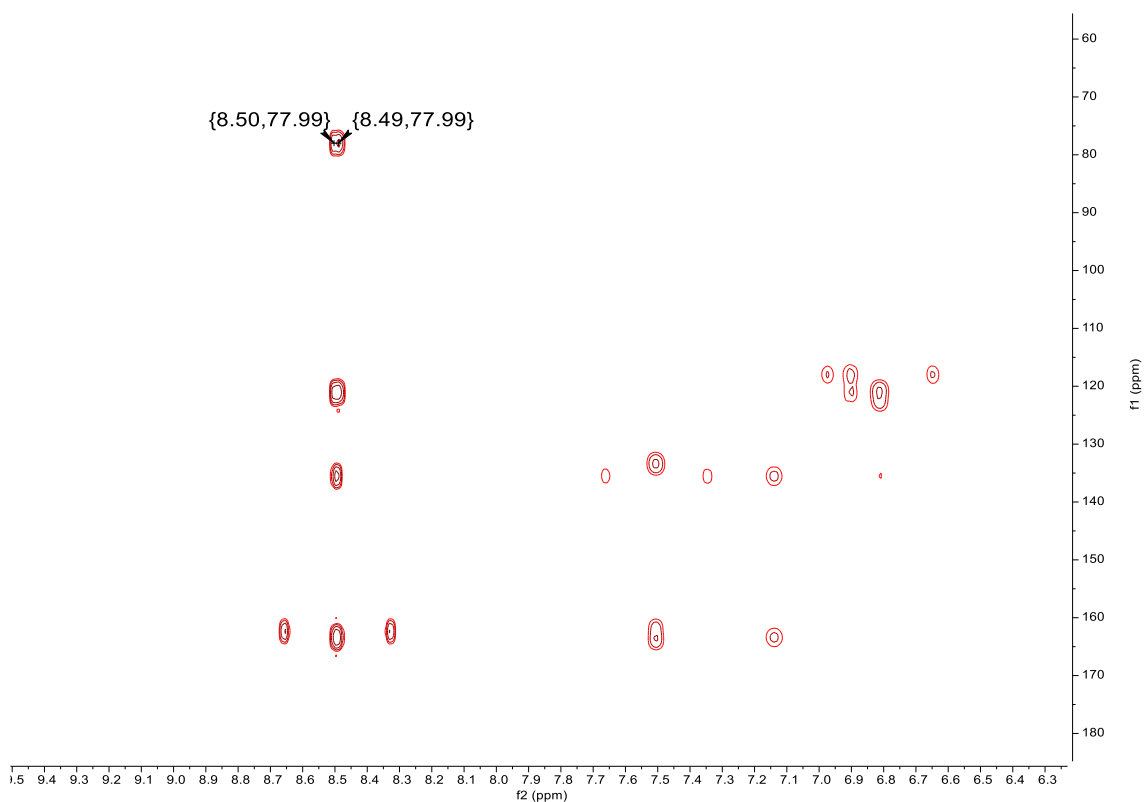


Figure S15. ¹H-¹³C HMBC (Acetone-*d*₆) spectrum of compound 3a.

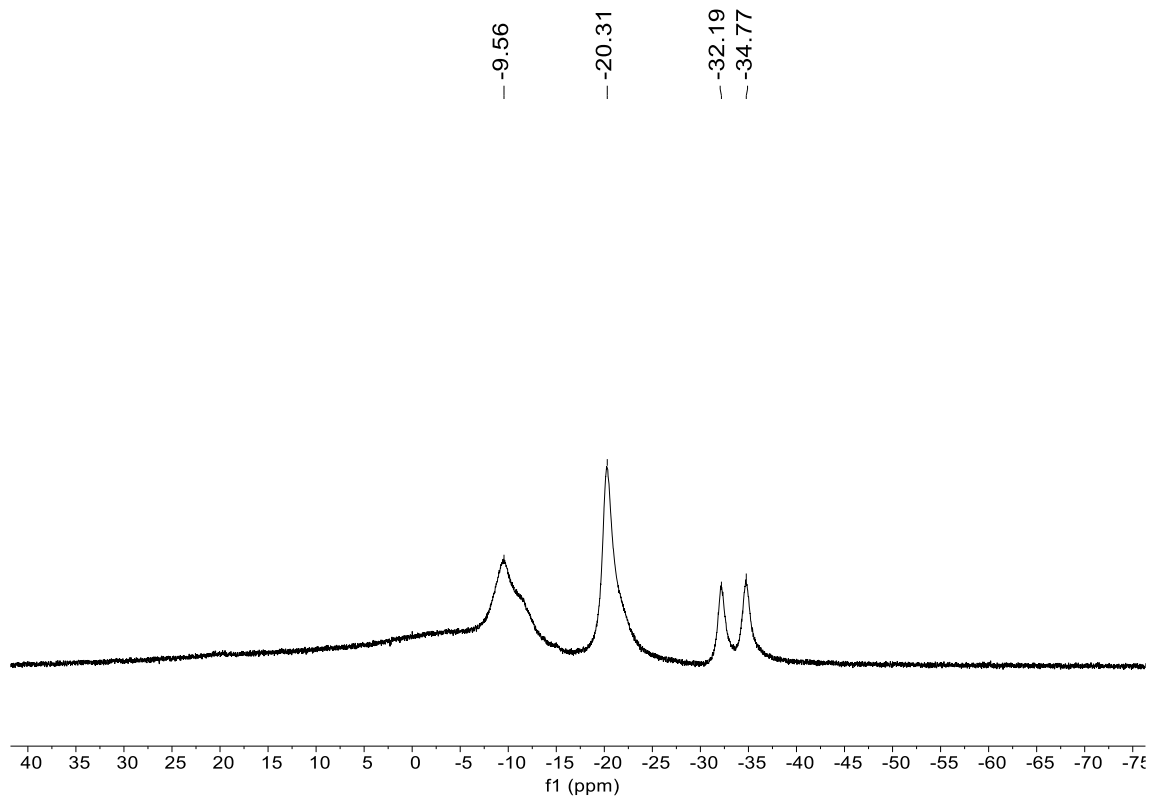


Figure S16. $^{11}\text{B}\{\text{H}\}$ NMR (Acetone- d_6 , 160.46 MHz) spectrum of compound **3a**.

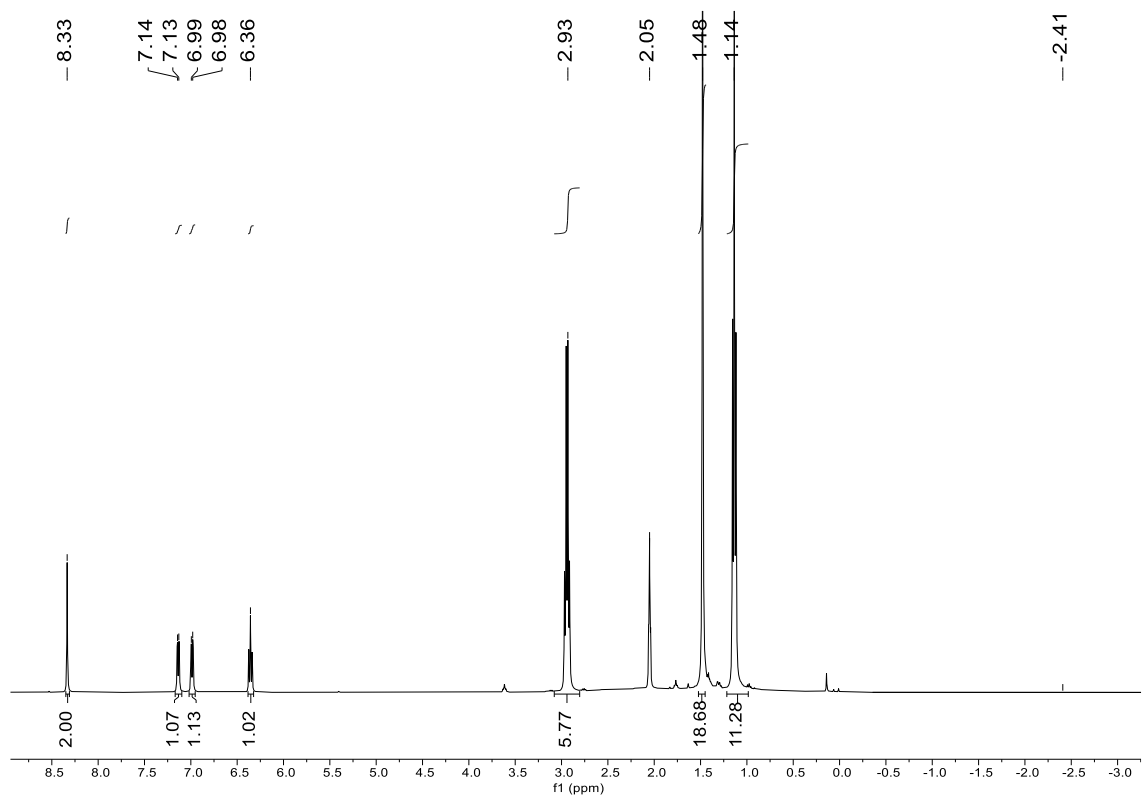


Figure S17. ^1H NMR (Acetone- d_6 , 400.13 MHz) spectrum of compound **3b**.

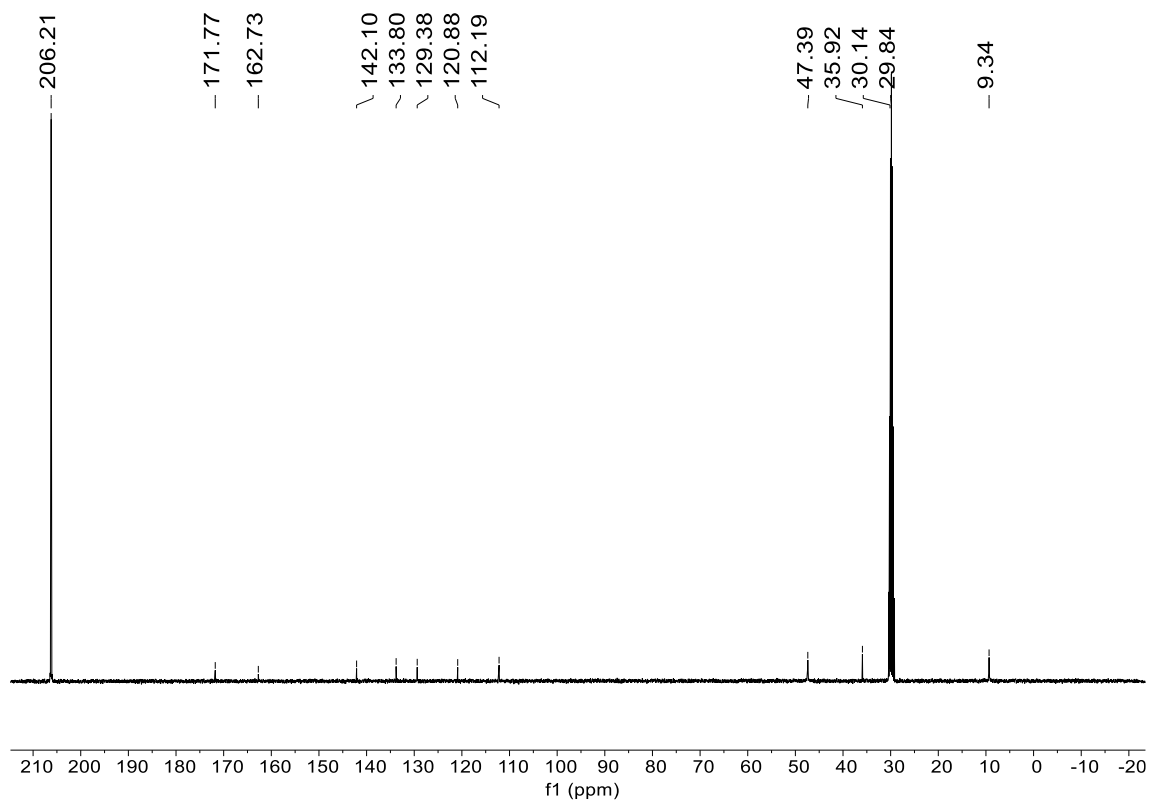


Figure S18. $^{13}\text{C}\{^1\text{H}\}$ NMR (Acetone- d_6 , 100.62 MHz) spectrum of compound **3b**.

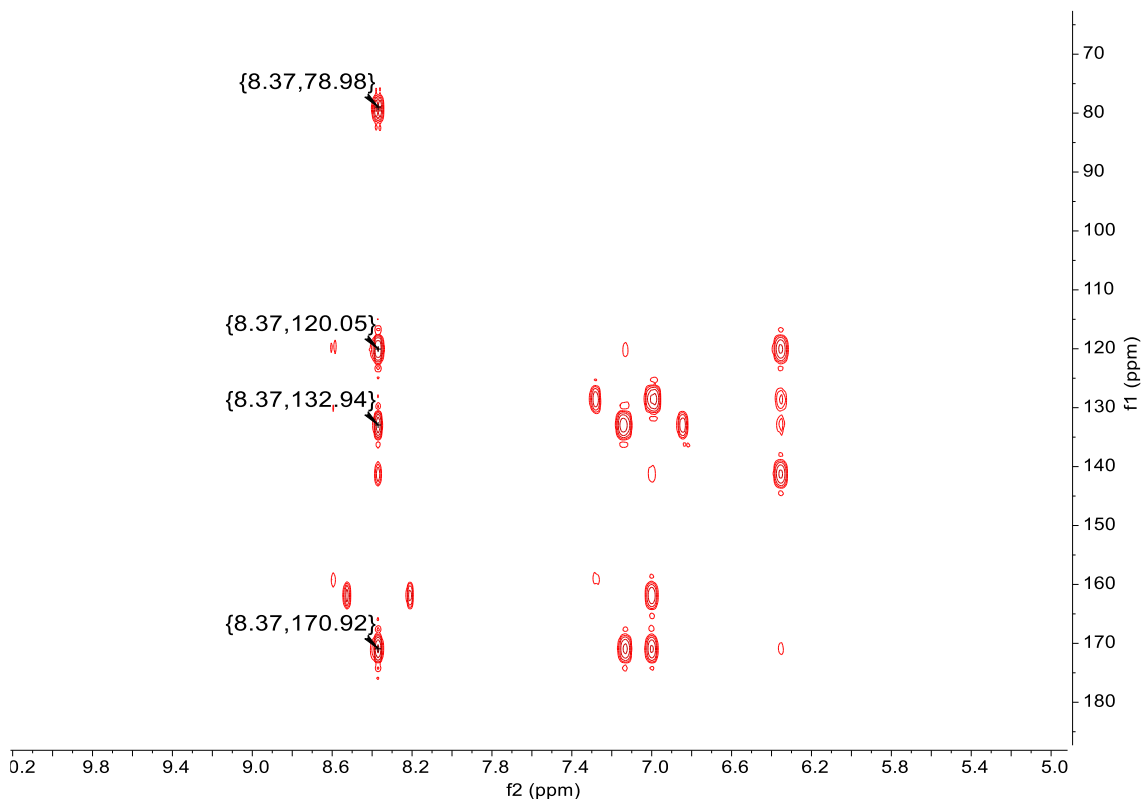
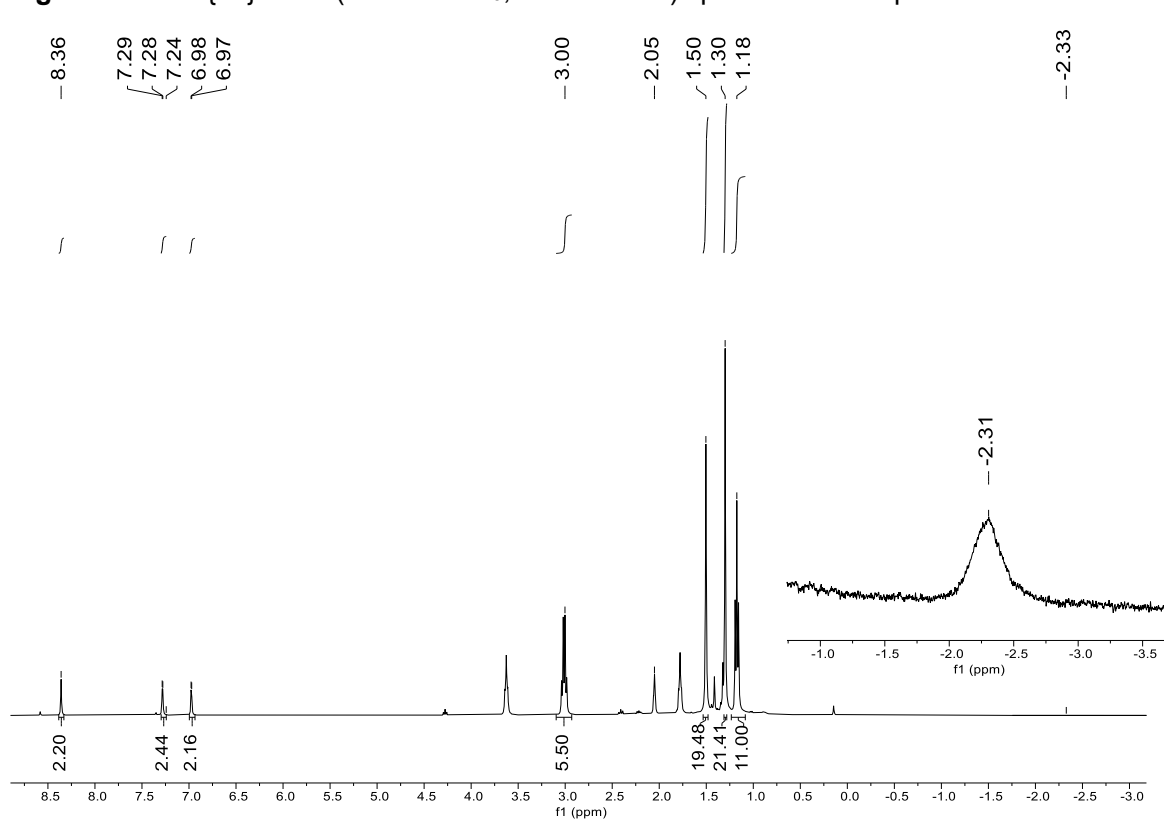
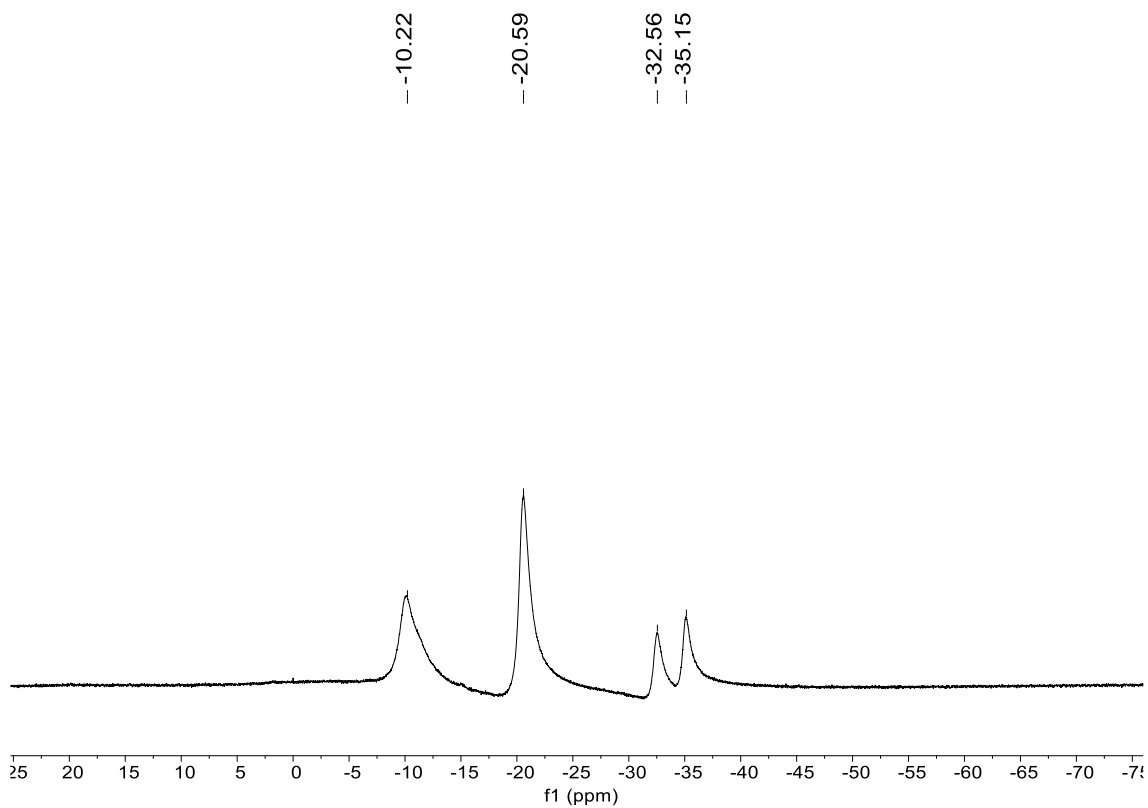


Figure S19. ^1H - ^{13}C HMBC (Acetone- d_6) spectrum of compound **3b**.



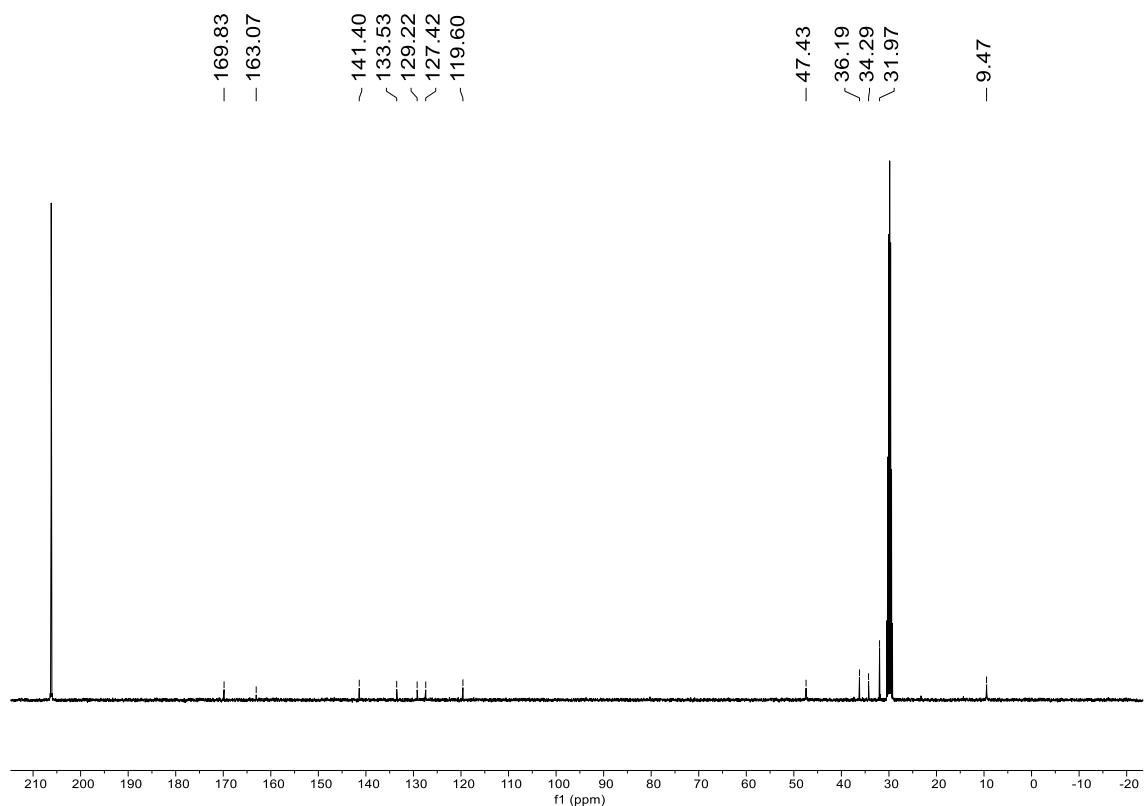


Figure S22. $^{13}\text{C}\{^1\text{H}\}$ NMR (Acetone- d_6 , 100.62 MHz) spectrum of compound **3c**.

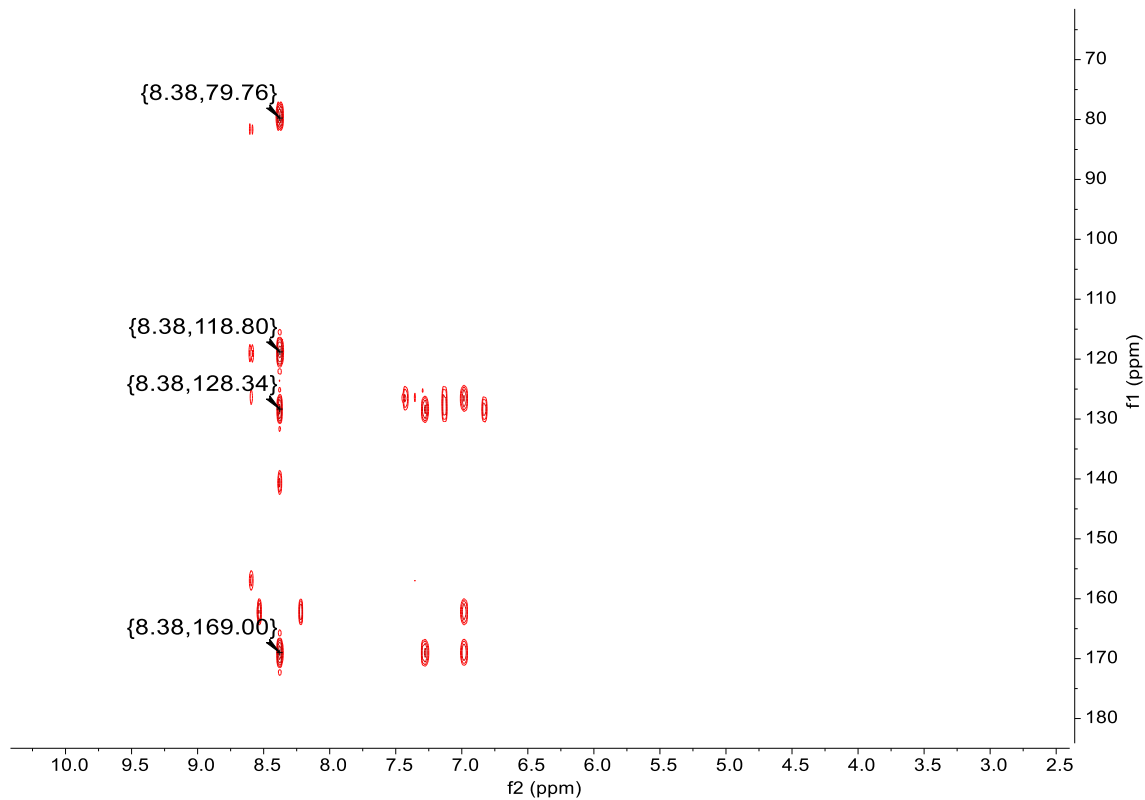


Figure S23. ^1H - ^{13}C HMBC (Acetone- d_6) spectrum of compound **3c**.

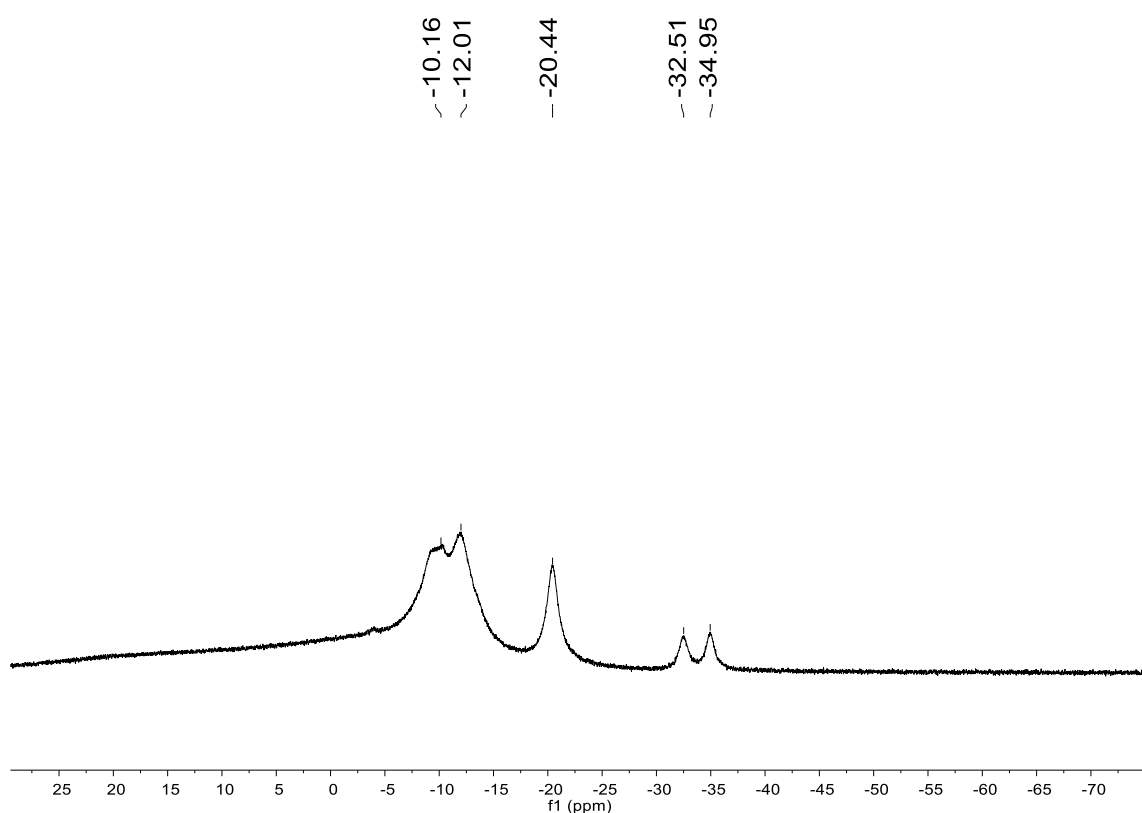


Figure S24. $^{11}\text{B}\{\text{H}\}$ NMR (Acetone- d_6 , 160.46 MHz) spectrum of compound **3c**.

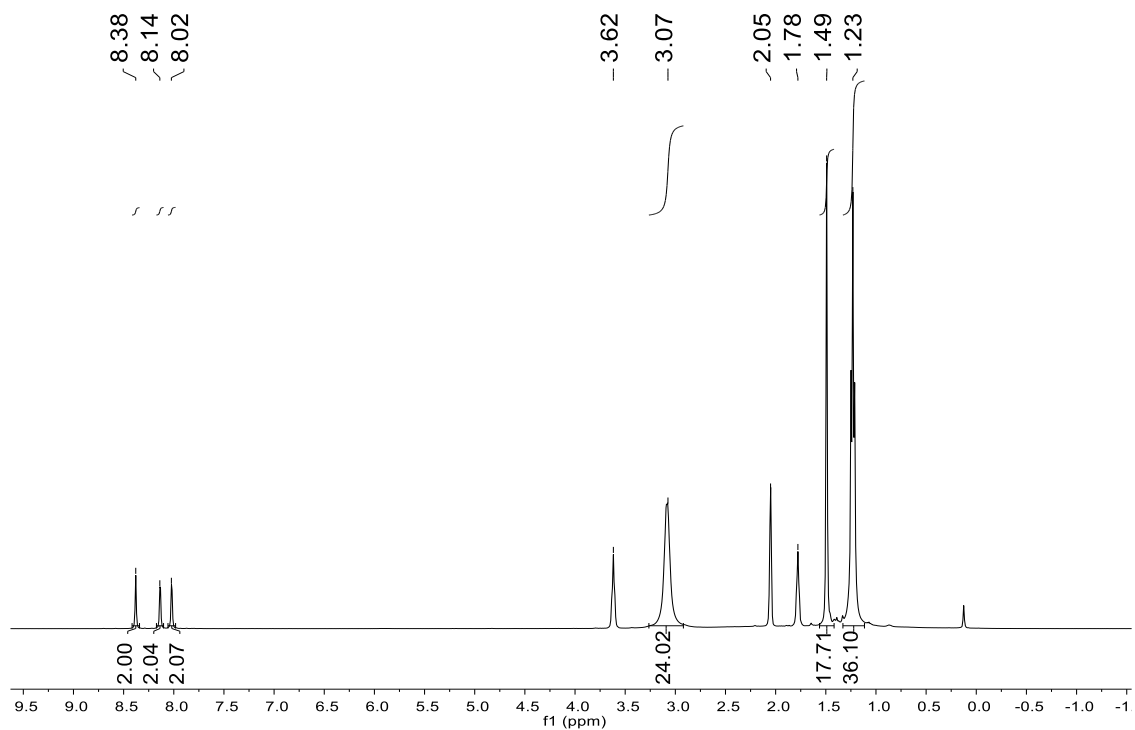


Figure S25. ^1H NMR (Acetone- d_6 , 400.13 MHz) spectrum of compound **3d**.

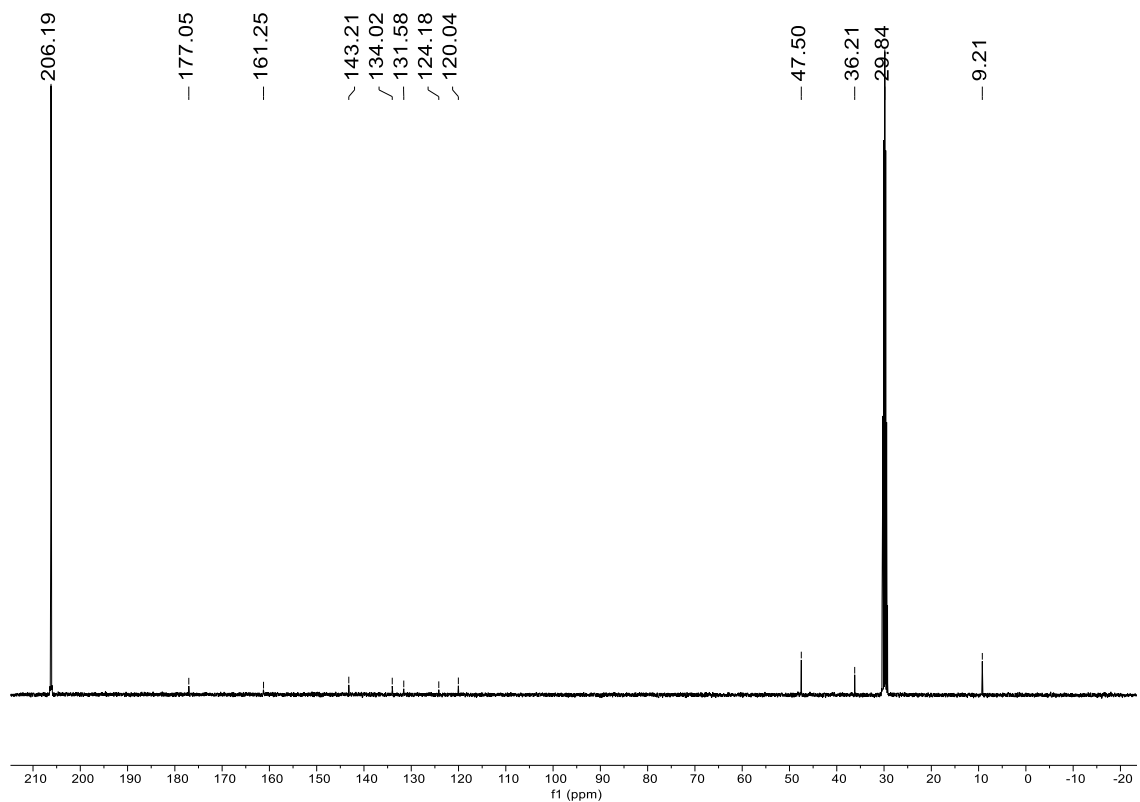


Figure S26. $^{13}\text{C}\{^1\text{H}\}$ NMR (Acetone- d_6 , 100.62 MHz) spectrum of compound **3d**.

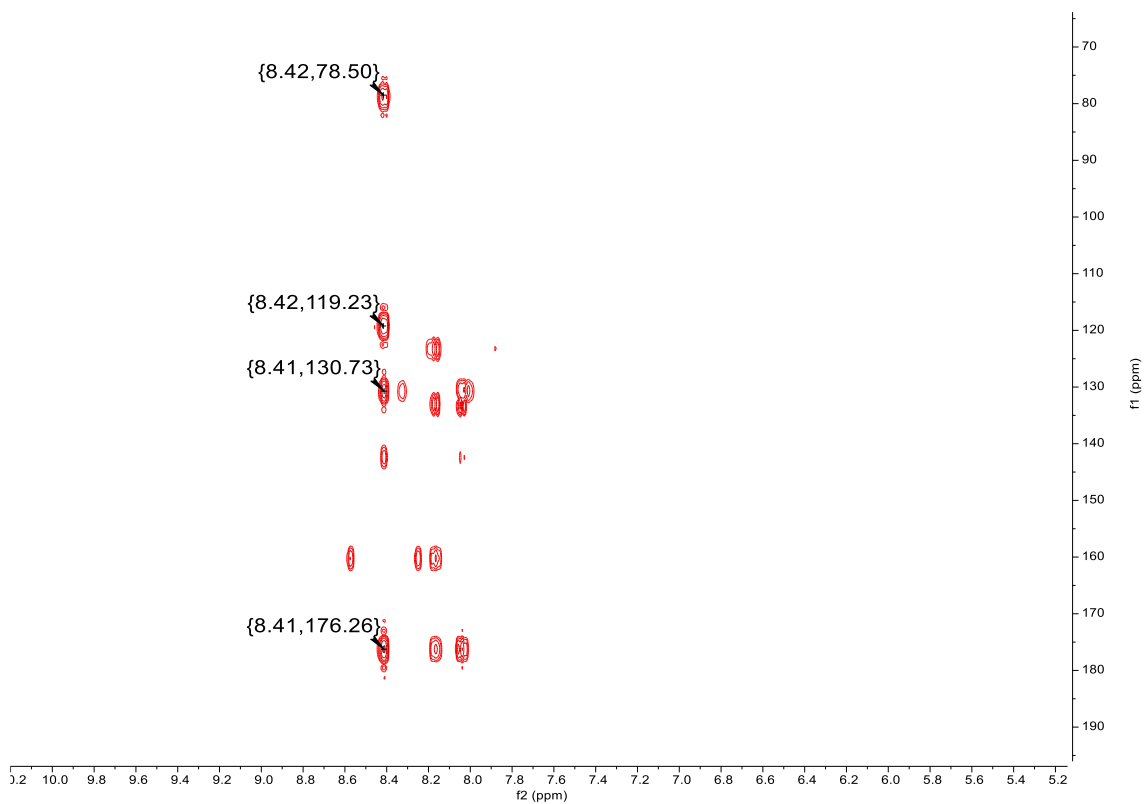


Figure S27. ^1H - ^{13}C HMBC (Acetone- d_6) spectrum of compound **3d**.

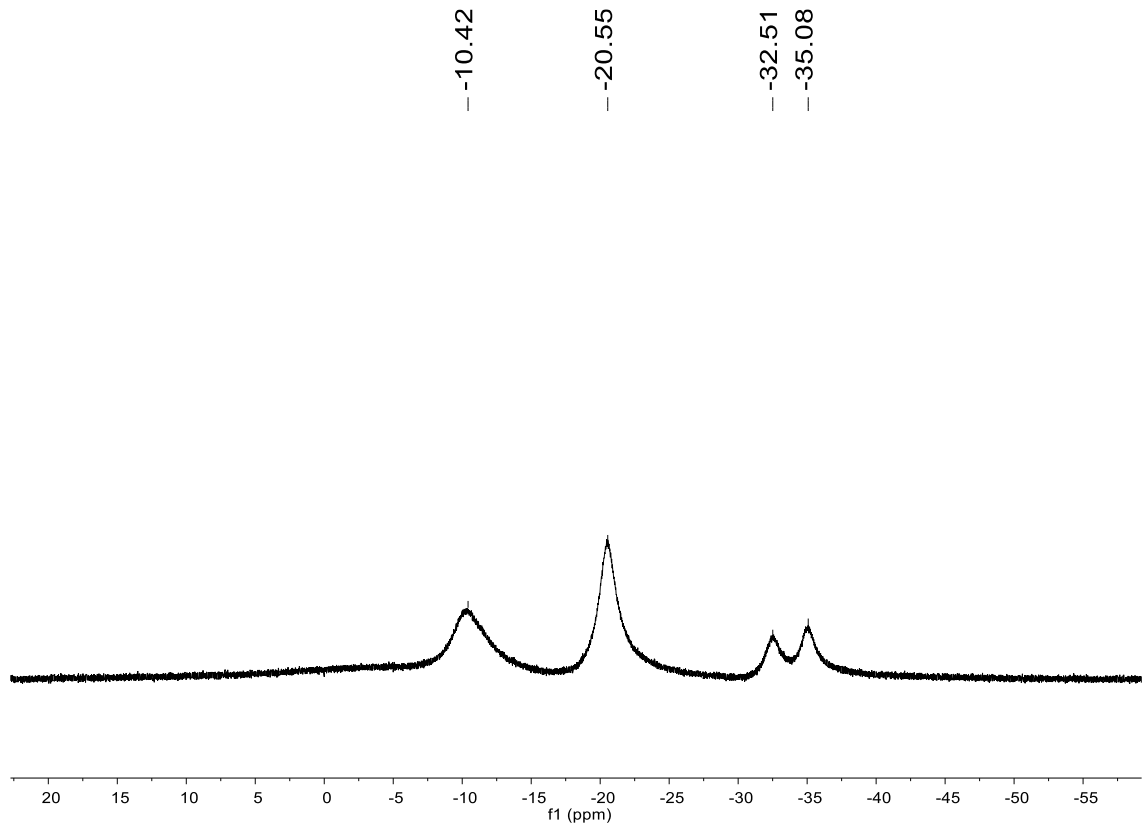


Figure S28. $^{11}\text{B}\{\text{H}\}$ NMR (Acetone- d_6 , 160.46 MHz) spectrum of compound **3d**.

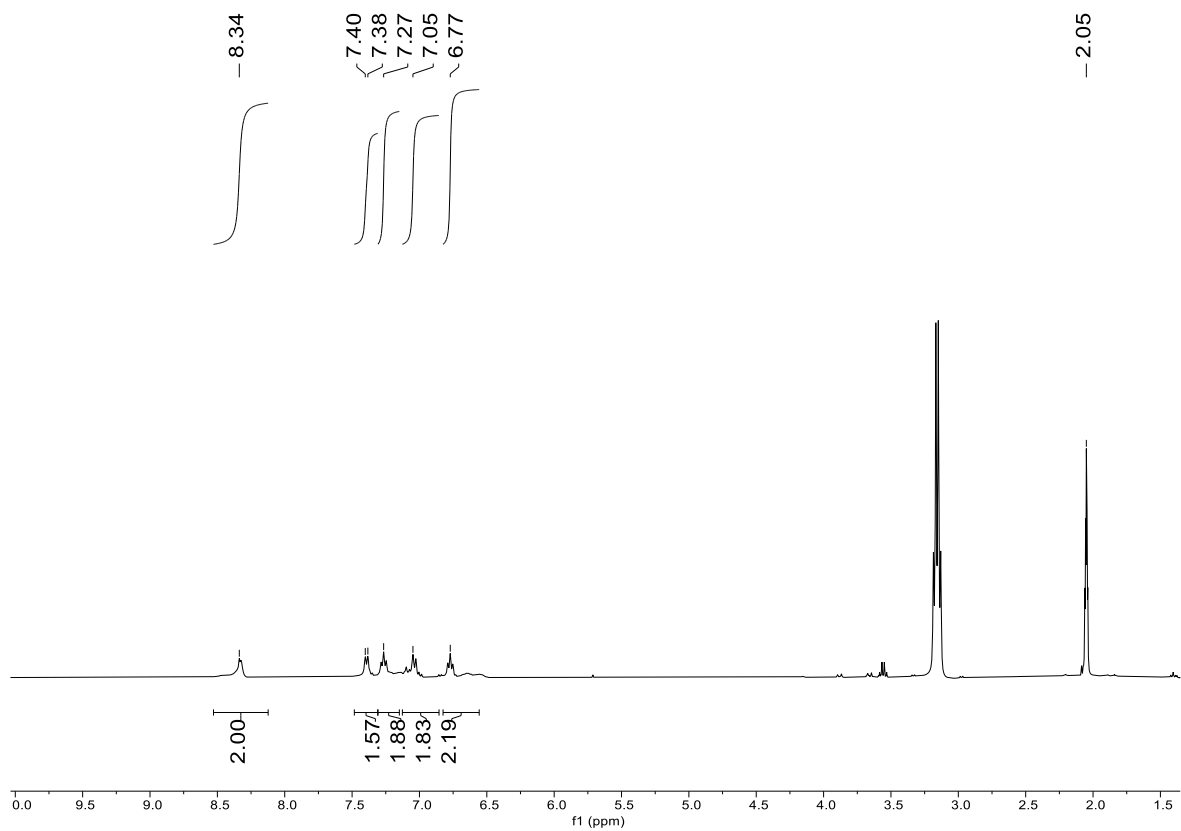


Figure S29. ^1H NMR (Acetone- d_6 , 400.13 MHz) spectrum of compound **4a**

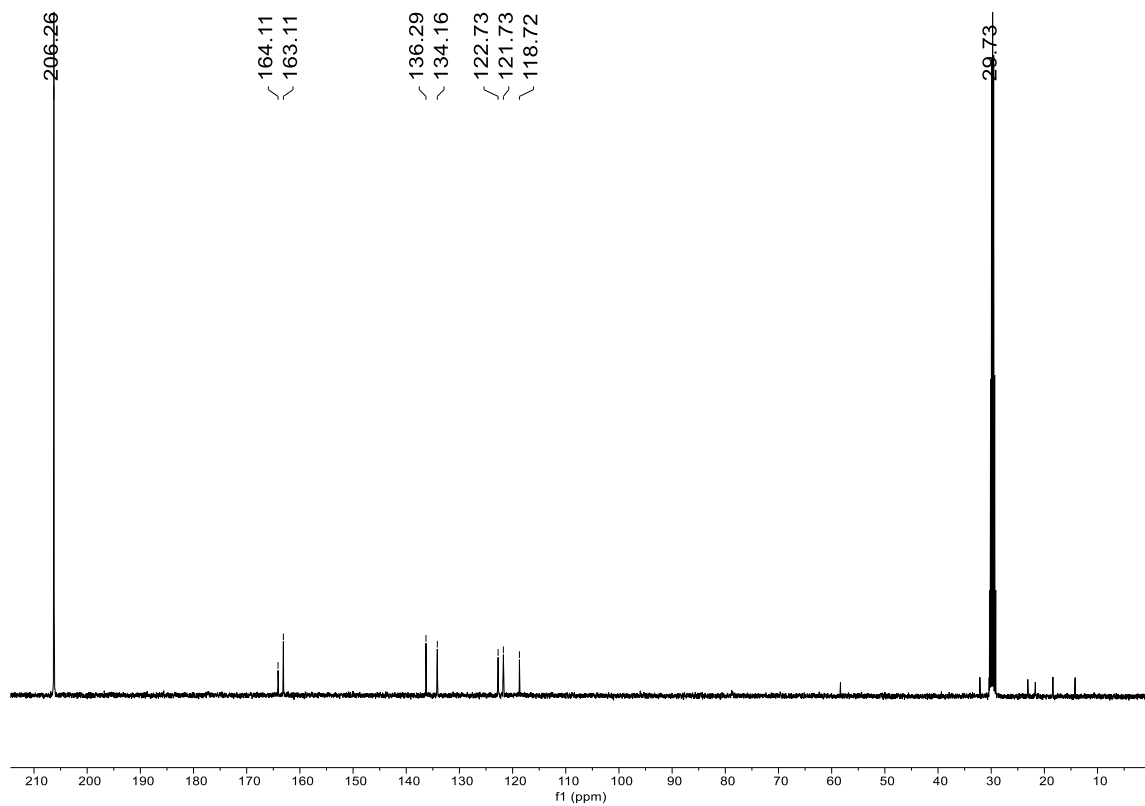


Figure S30. $^{13}\text{C}\{\text{H}\}$ NMR (Acetone- d_6 , 100.62 MHz) spectrum of compound **4a**.

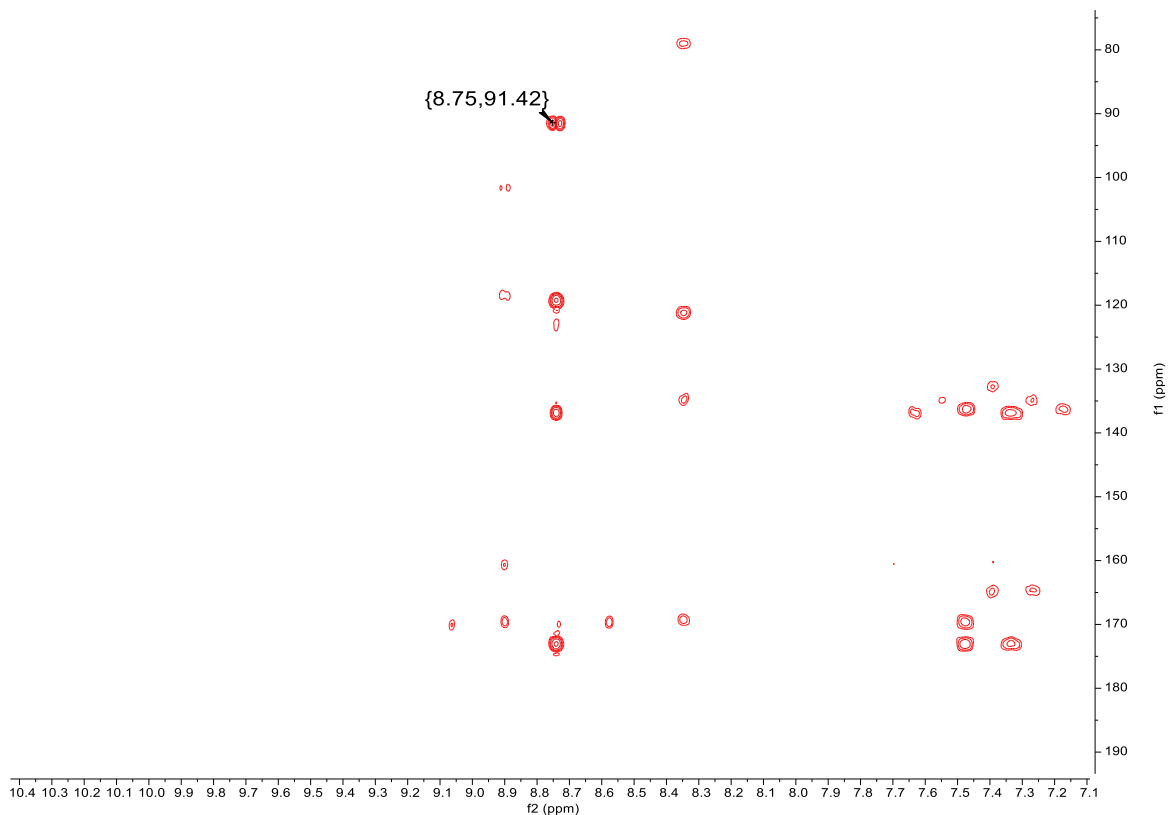


Figure S31. ^1H - ^{13}C HMBC (Acetone- d_6) spectrum of compound **4a**

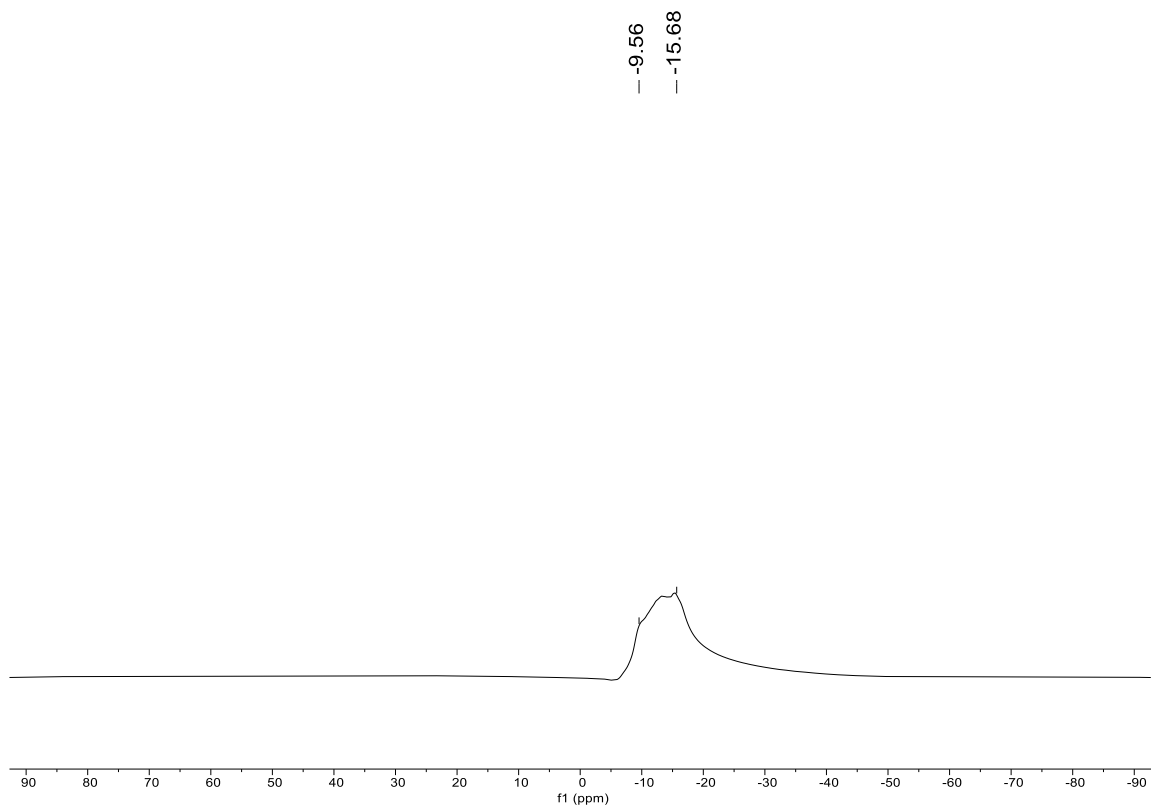


Figure S32. $^{11}\text{B}\{\text{H}\}$ NMR (Acetone- d_6 , 160.46 MHz) spectrum of compound **4a**

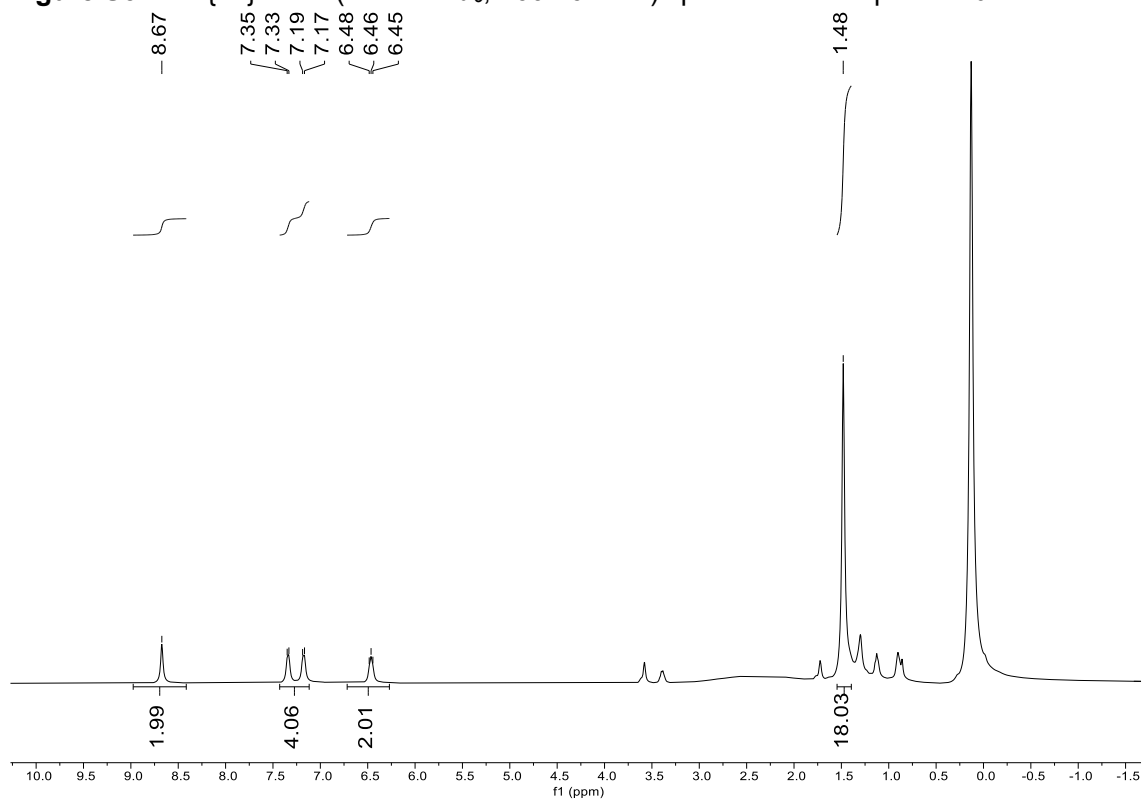


Figure S33. ^1H NMR (Acetone- d_6 , 400.13 MHz) spectrum of compound **4b**

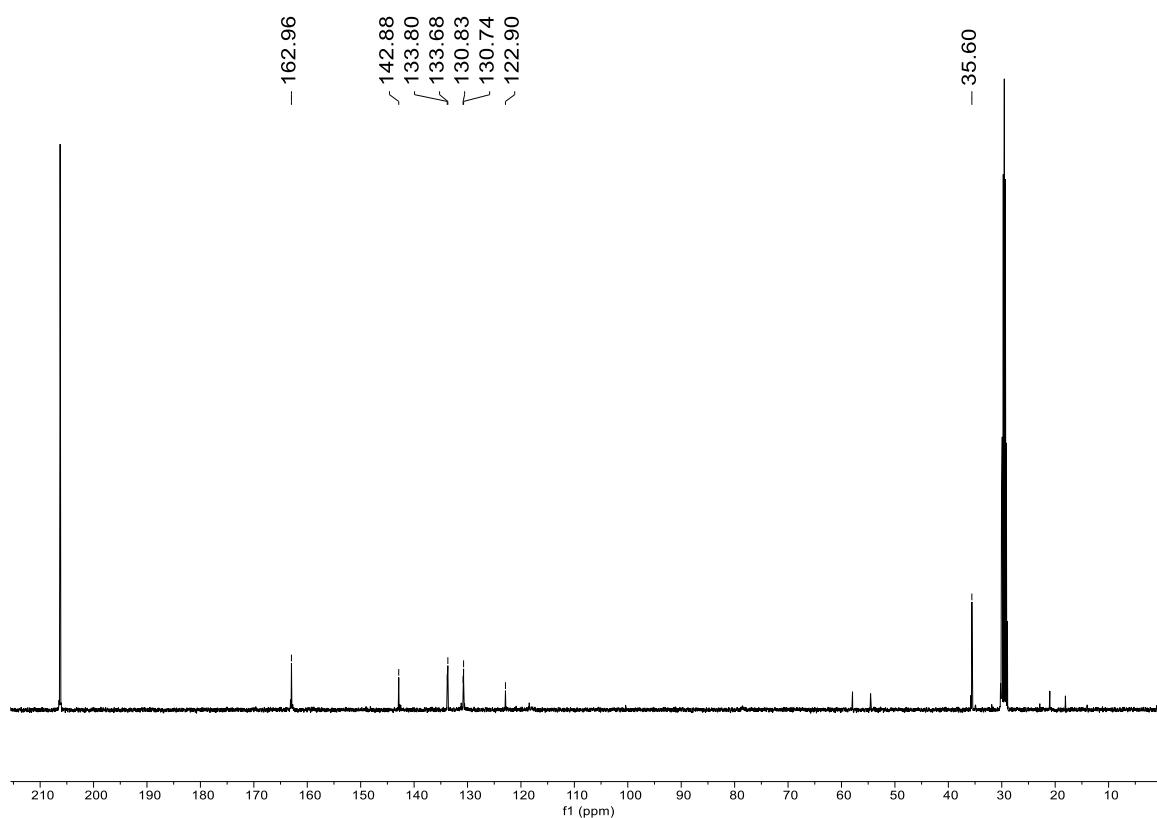


Figure S34. $^{13}\text{C}\{\text{H}\}$ NMR (Acetone- d_6 , 100.62 MHz) spectrum of compound **4b**

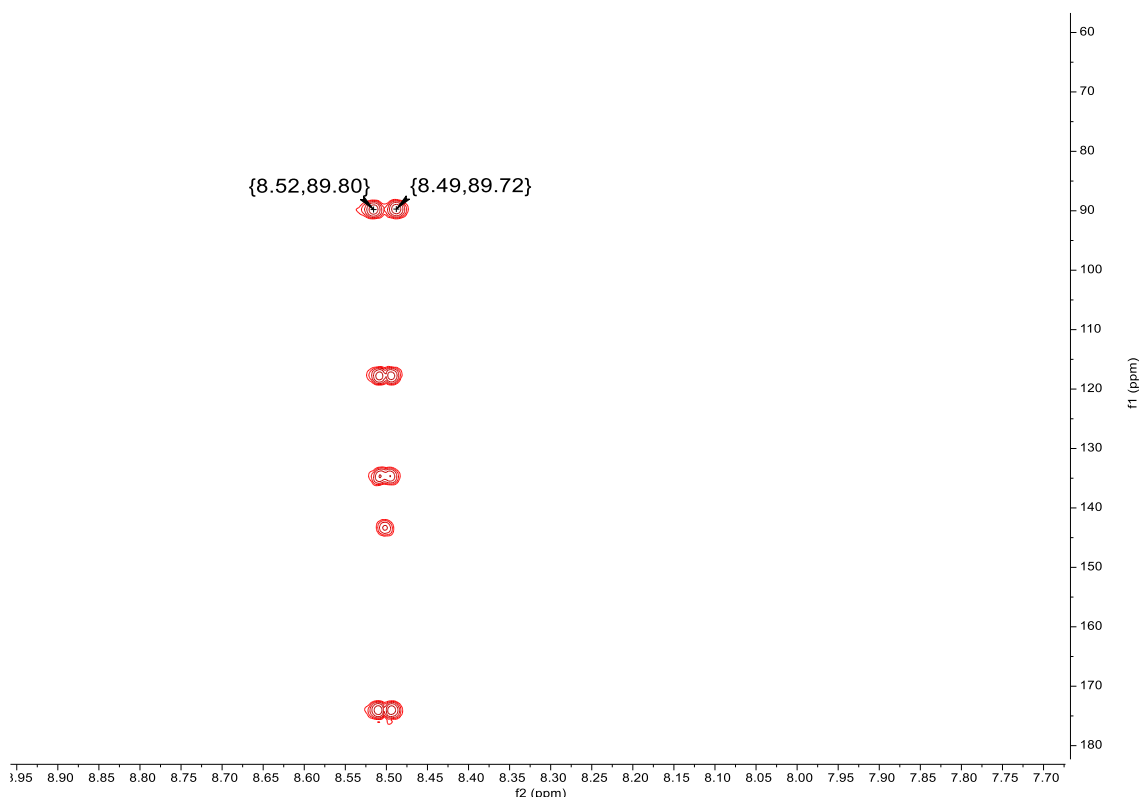


Figure S35. ^1H - ^{13}C HMBC (Acetone- d_6) spectrum of compound **4b**

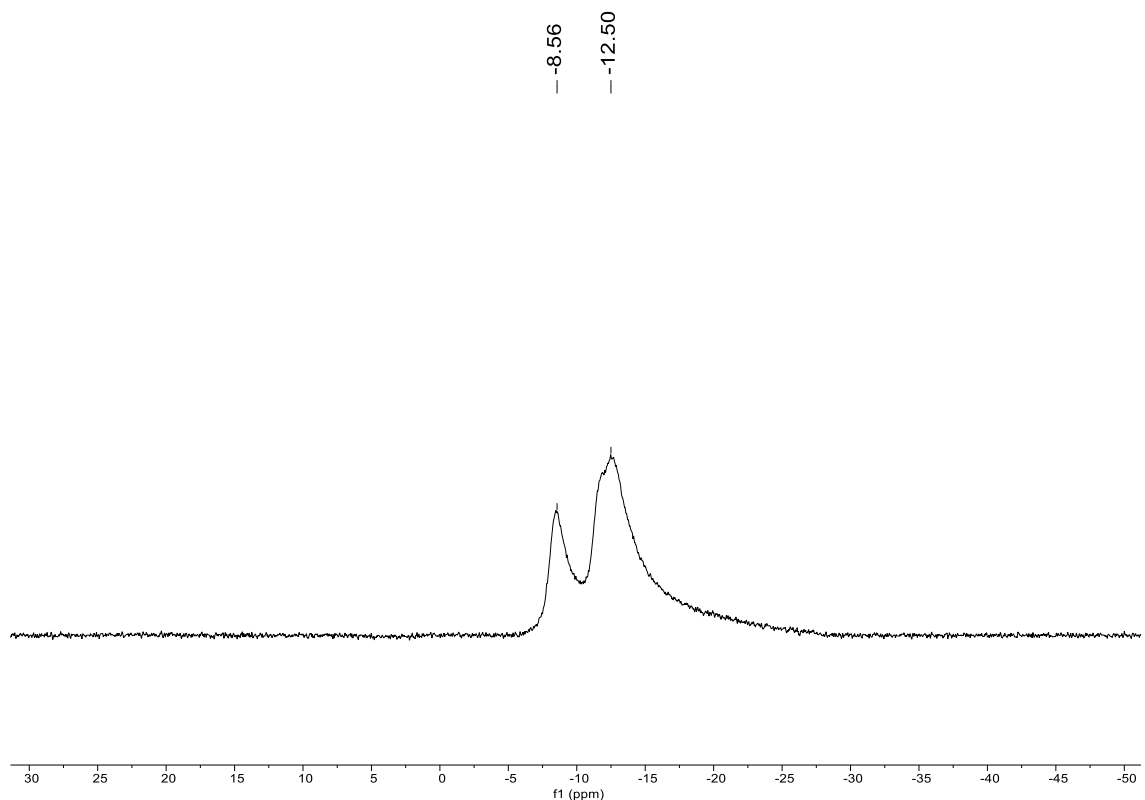


Figure S36. ¹¹B{¹H} NMR (Acetone-*d*₆, 160.46 MHz) spectrum of compound **4b**

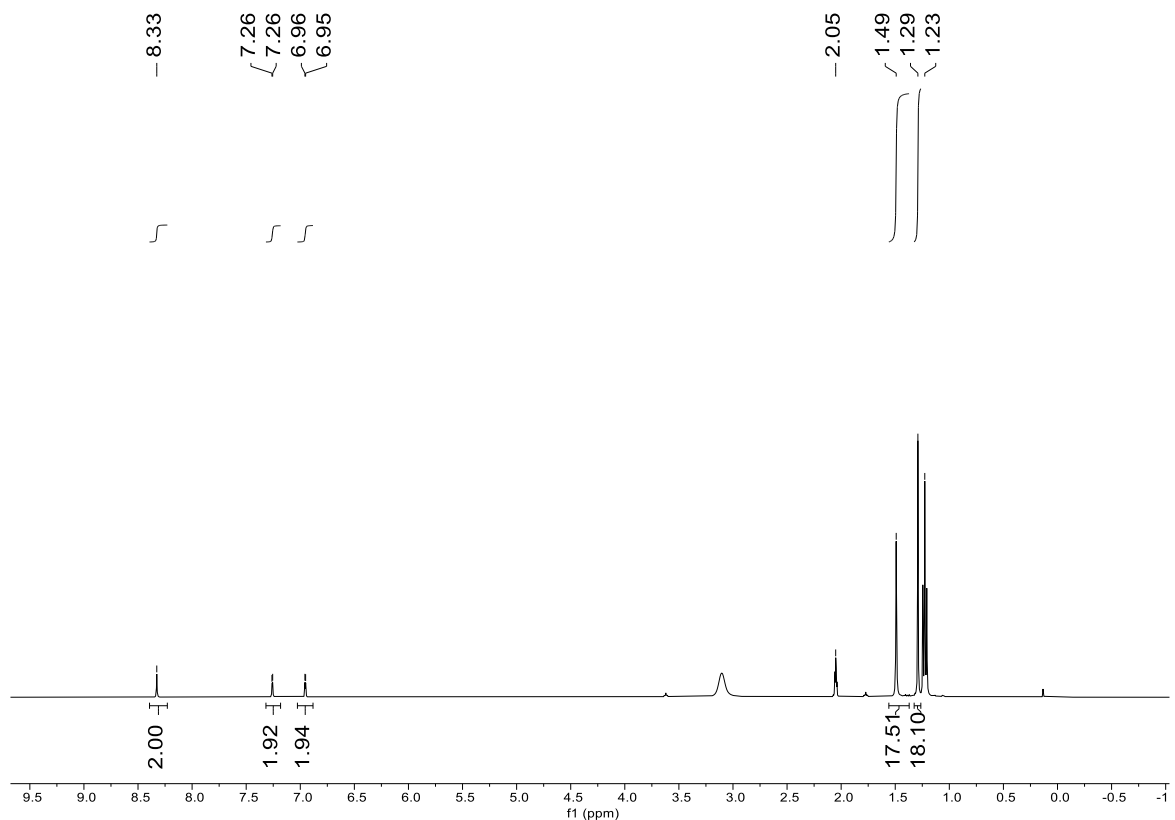


Figure S37. ¹H NMR (Acetone-*d*₆, 400.13 MHz) spectrum of compound **4c**

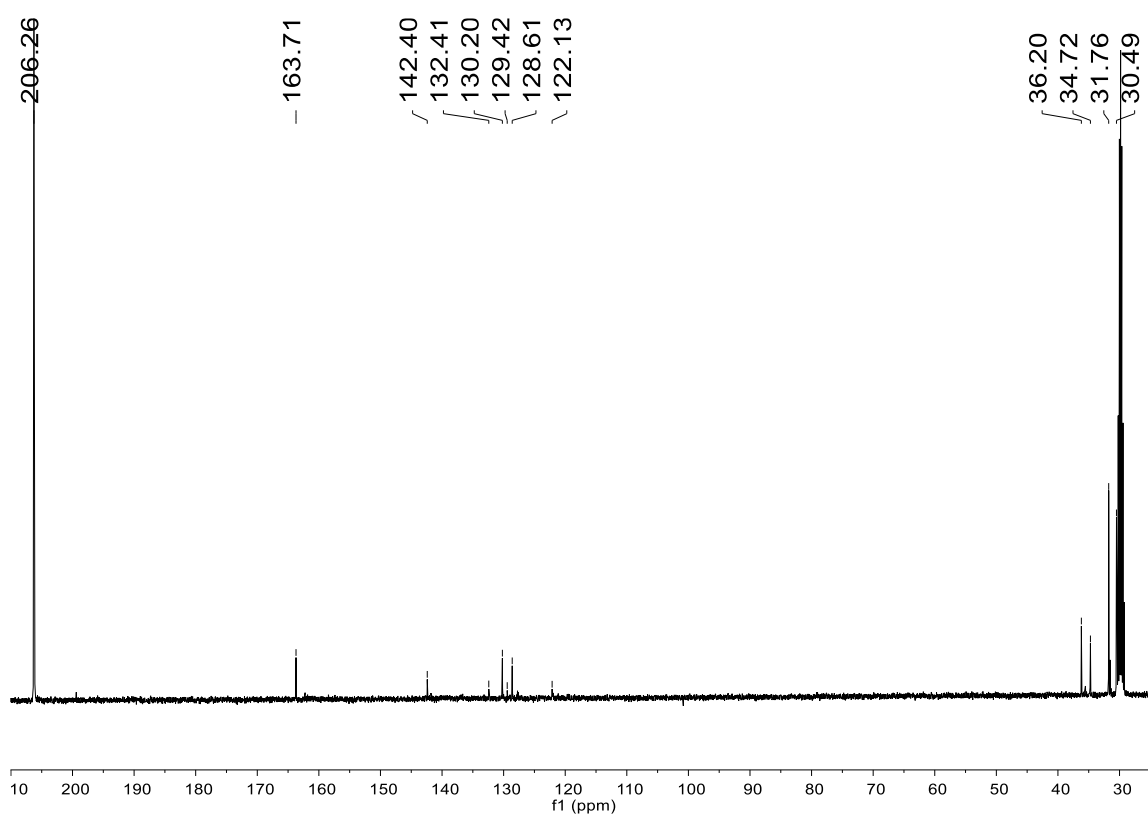


Figure S38. ¹³C{¹H} NMR (Acetone-*d*₆, 100.62 MHz) spectrum of compound **4c**

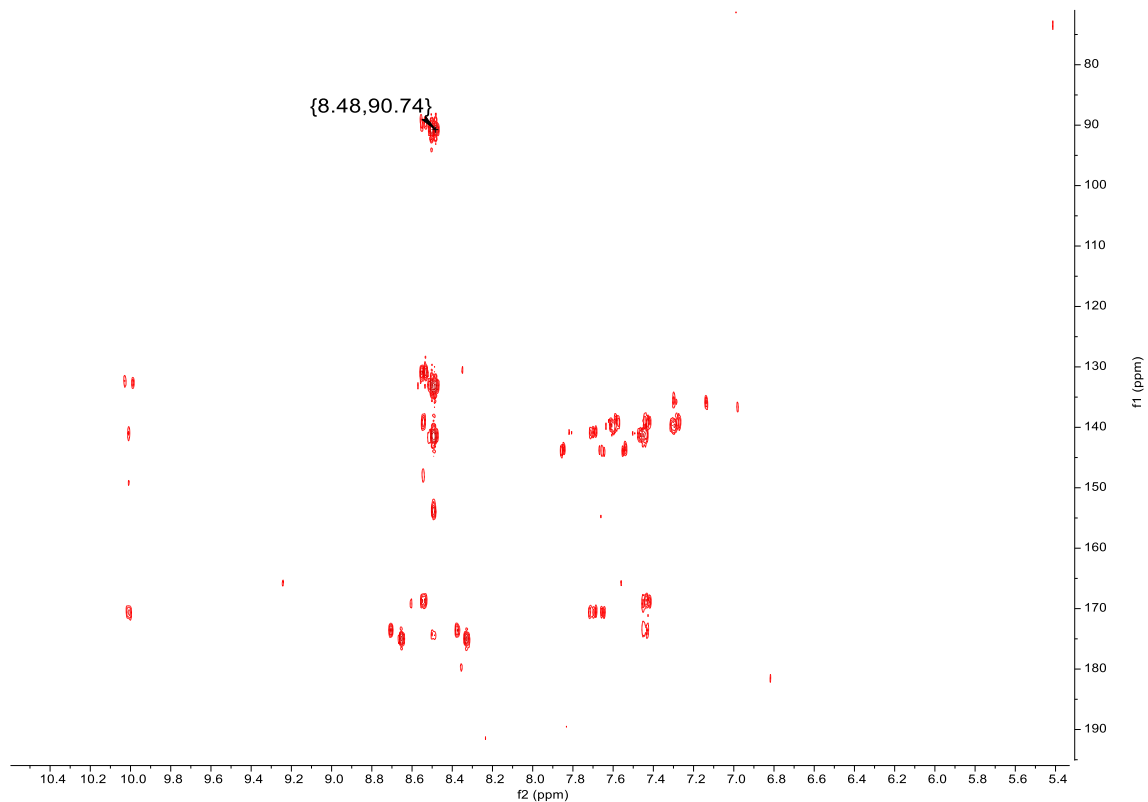


Figure S39 ¹¹H-¹³C HMBC (Acetone-*d*₆) spectrum of compound **4c**

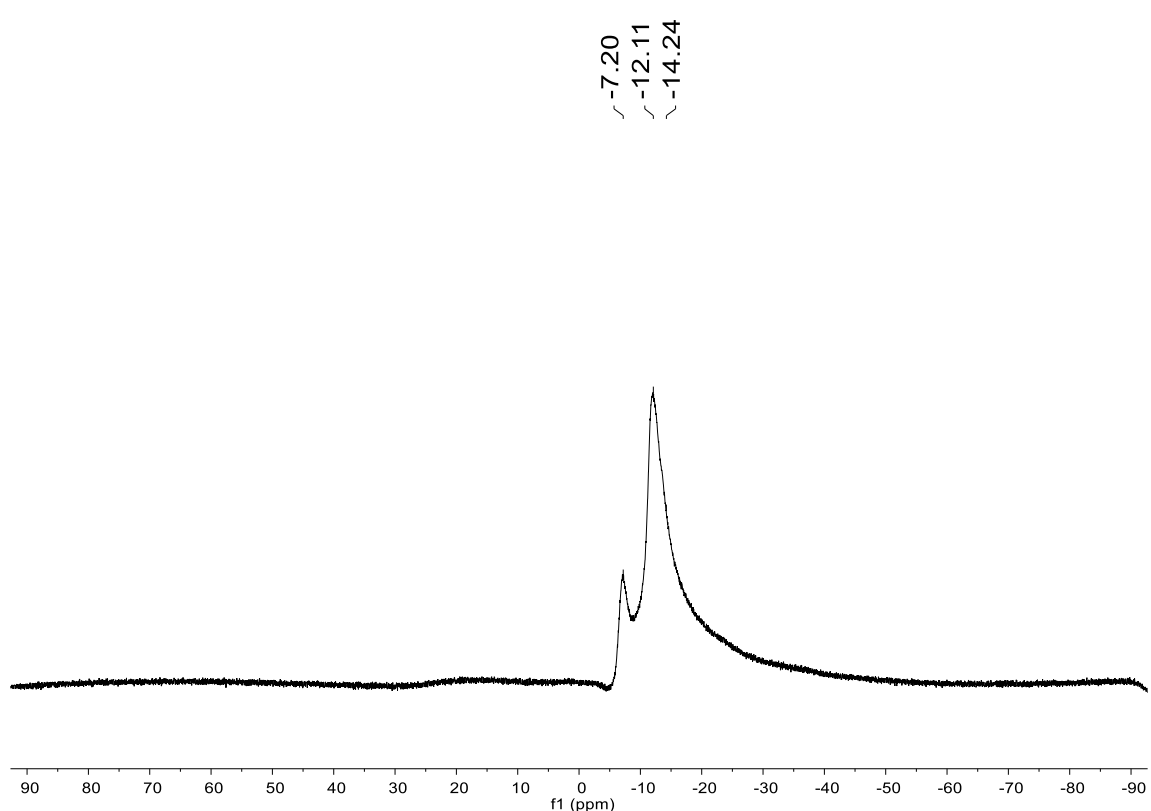


Figure S40. ¹¹B{¹H} NMR (Acetone-*d*₆, 160.46 MHz) spectrum of compound **4c**

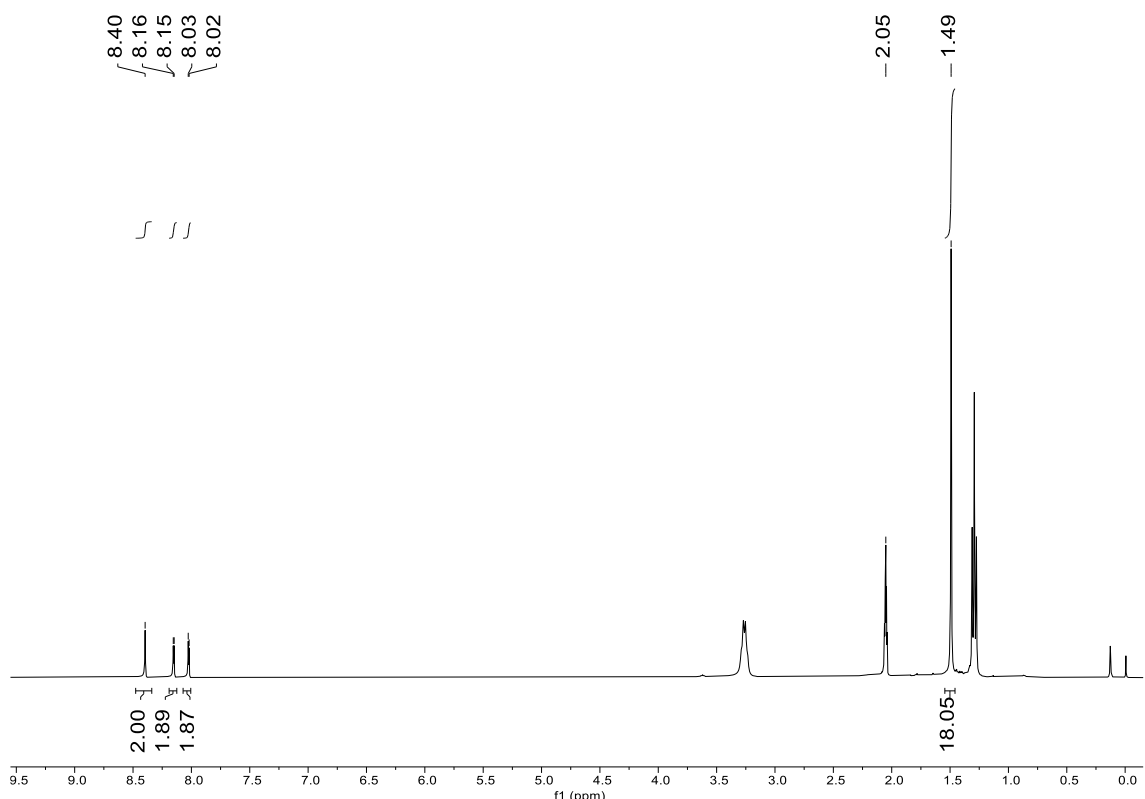


Figure S41. ¹H NMR (Acetone-*d*₆, 400.13 MHz) spectrum of compound **4d**

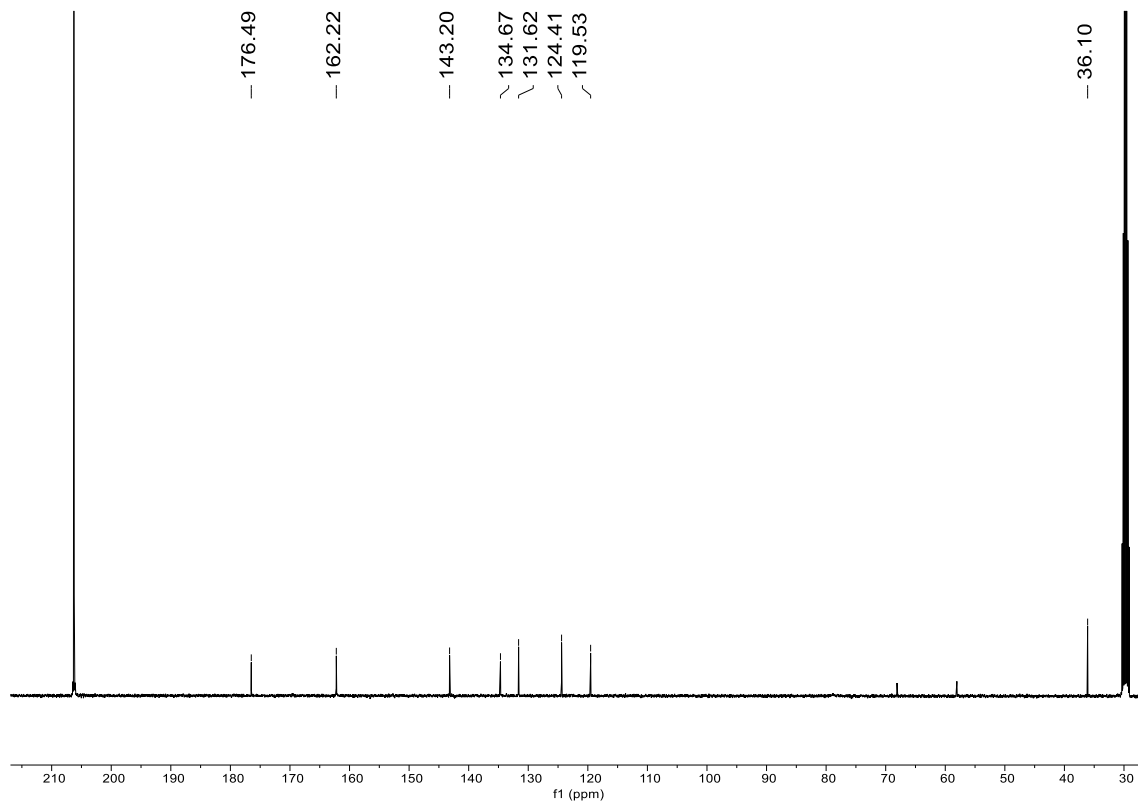


Figure S42. $^{13}\text{C}\{\text{H}\}$ NMR (Acetone- d_6 , 100.62 MHz) spectrum of compound **4d**

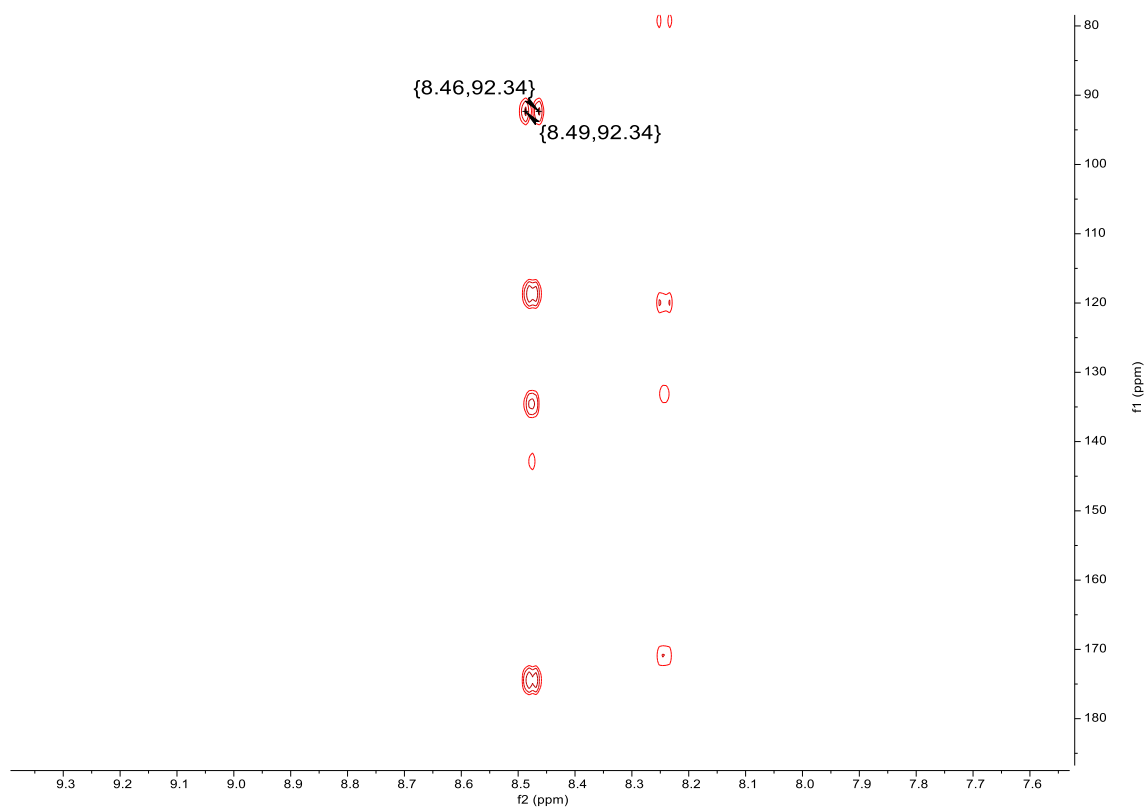


Figure S43. ^1H - ^{13}C HMBC (Acetone- d_6) spectrum of compound **4d**

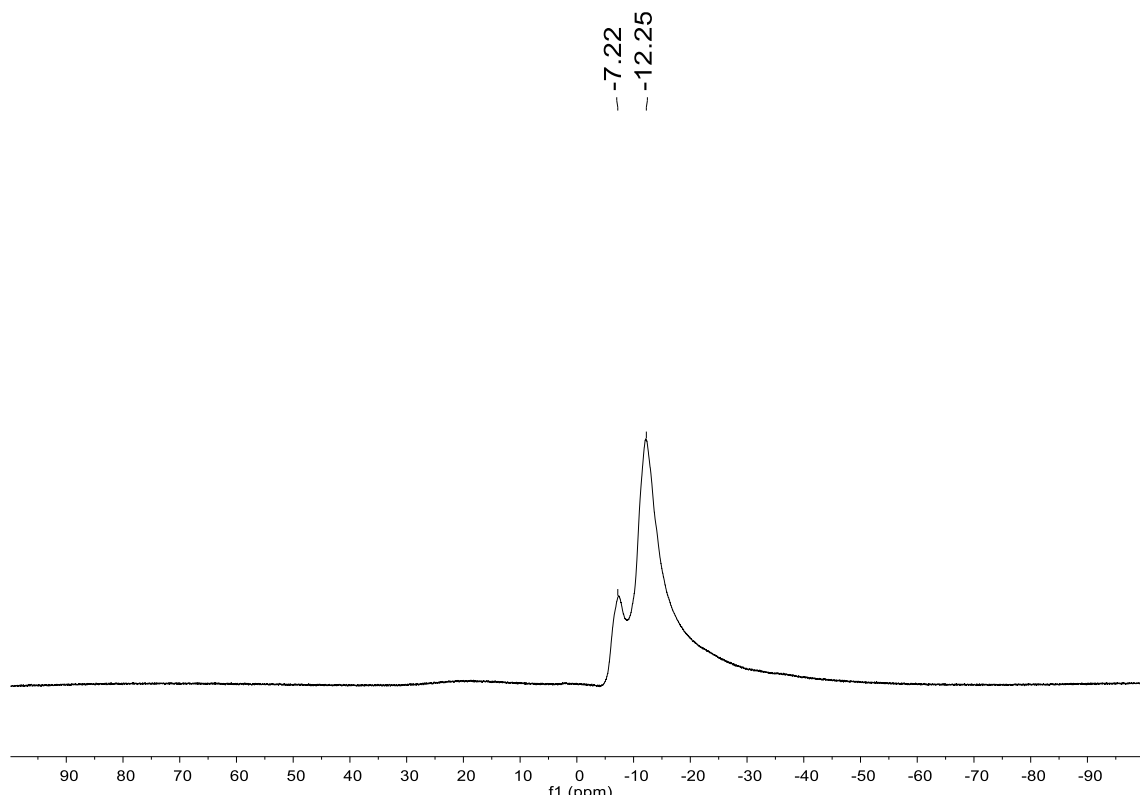


Figure S44. $^{11}\text{B}\{\text{H}\}$ NMR (Acetone- d_6 , 160.46 MHz) spectrum of compound **4d**

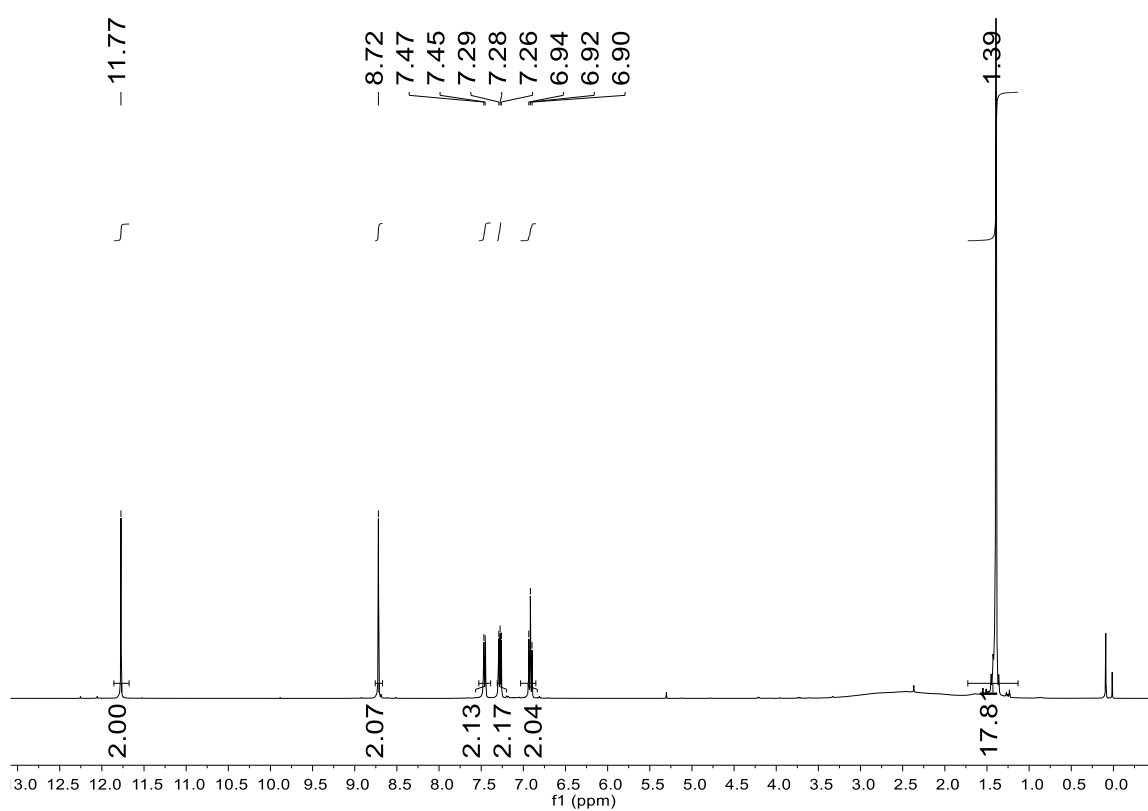


Figure S45. ^1H NMR (CDCl_3 , 400.13 MHz) spectrum of compound **1b**.

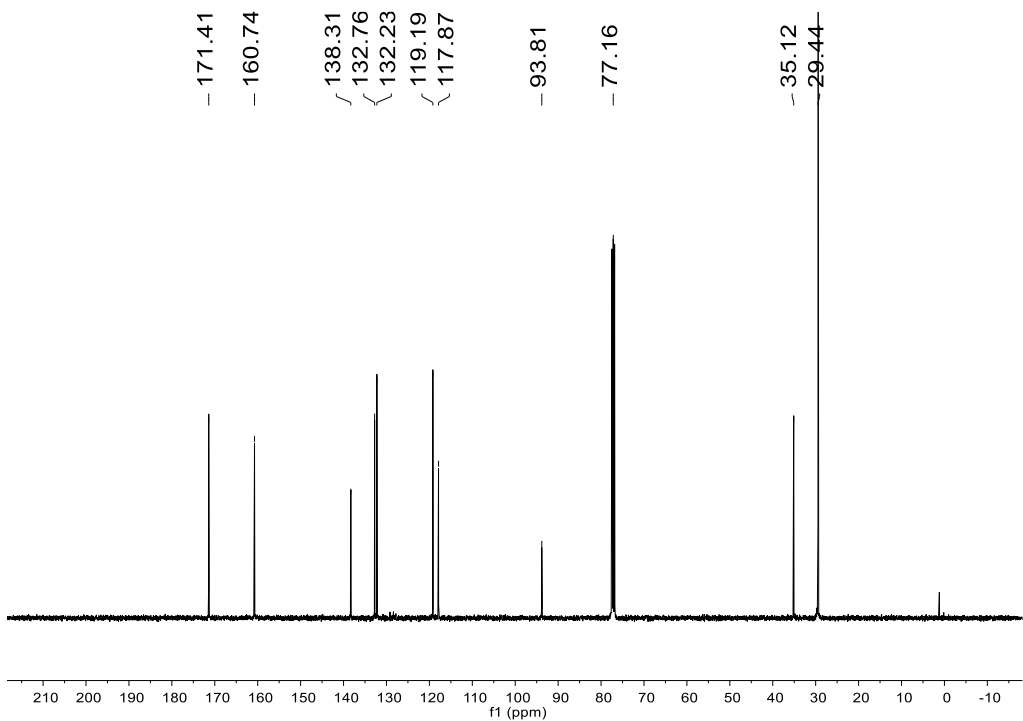


Figure S46. $^{13}\text{C}\{^1\text{H}\}$ NMR (CDCl_3 , 100.62 MHz) spectrum of compound **1b**.

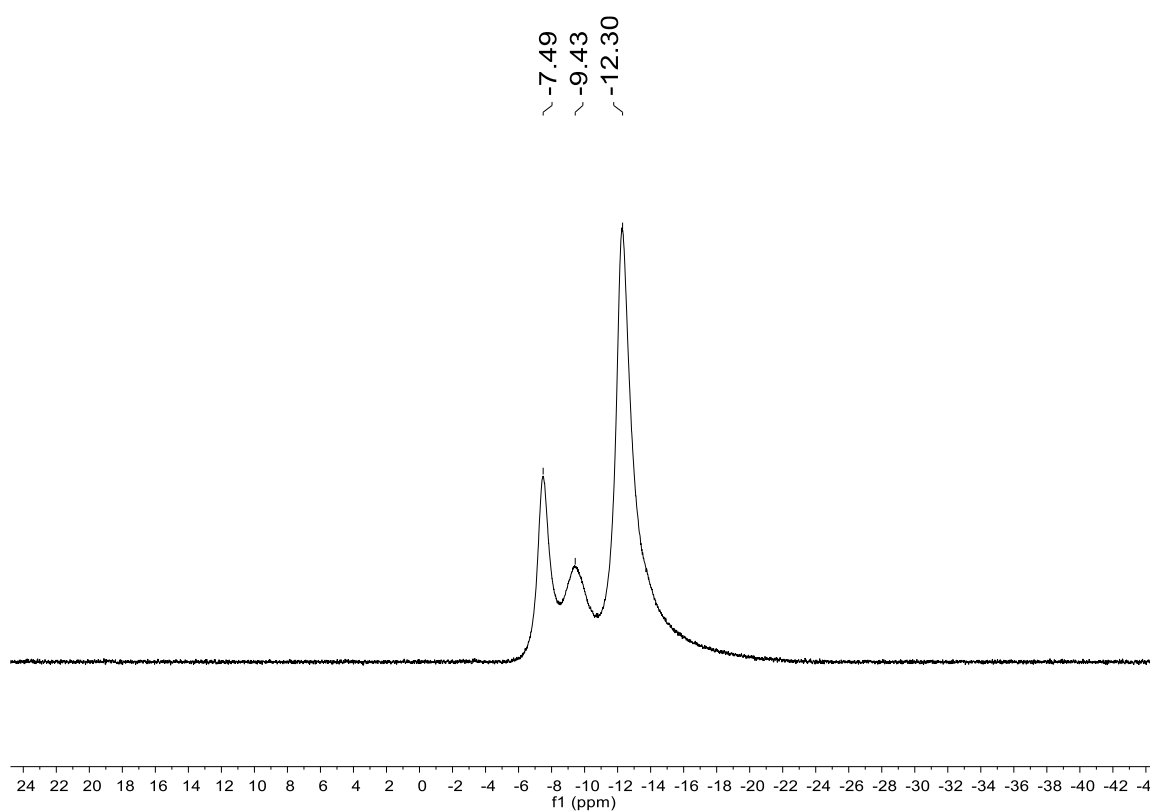


Figure S47. $^{11}\text{B}\{^1\text{H}\}$ NMR (CDCl_3 , 160.46 MHz) spectrum of compound **1b**

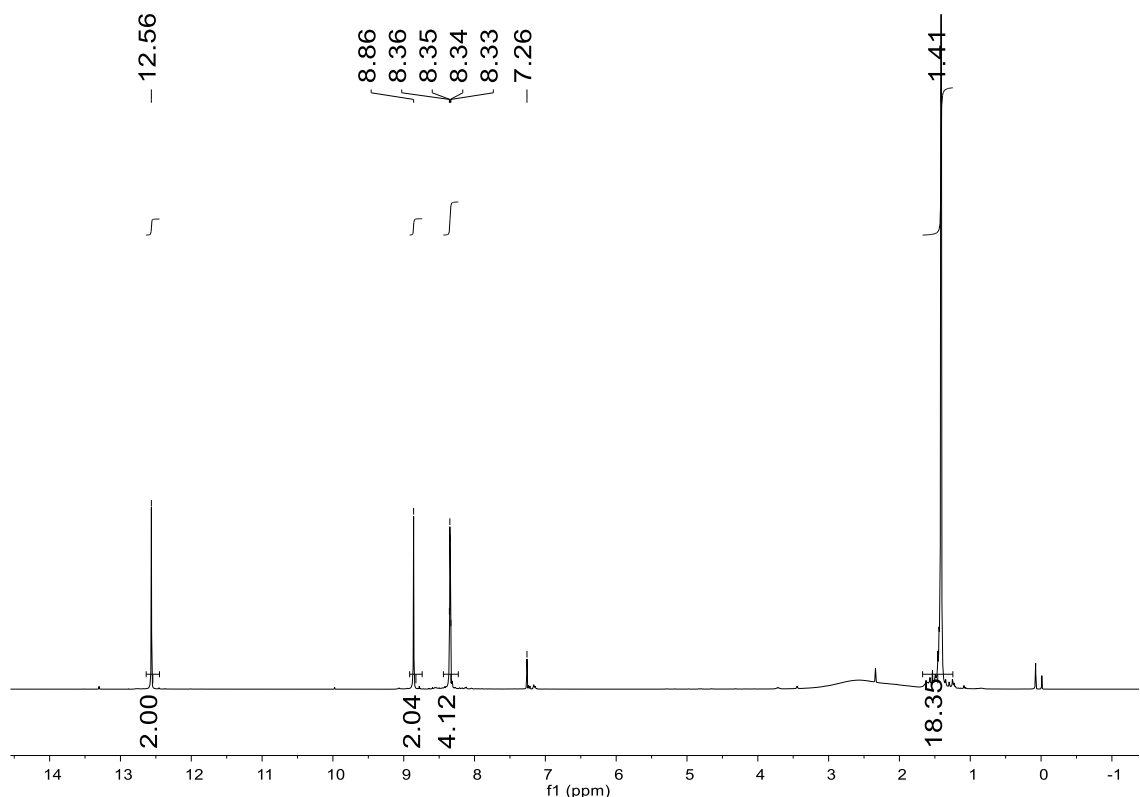


Figure S48. ^1H NMR (CDCl_3 , 400.13 MHz) spectrum of compound **1d**.

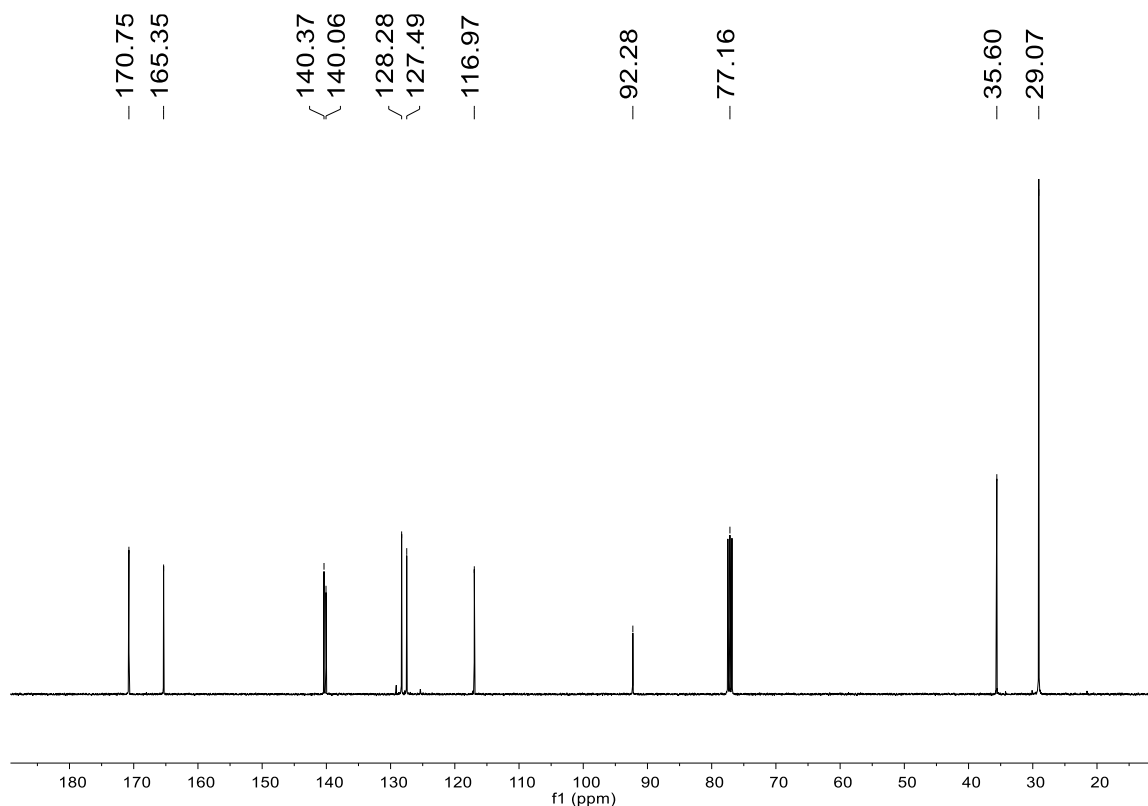


Figure S49. $^{13}\text{C}\{\text{H}\}$ NMR (CDCl_3 , 100.62 MHz) spectrum of compound **1d**.

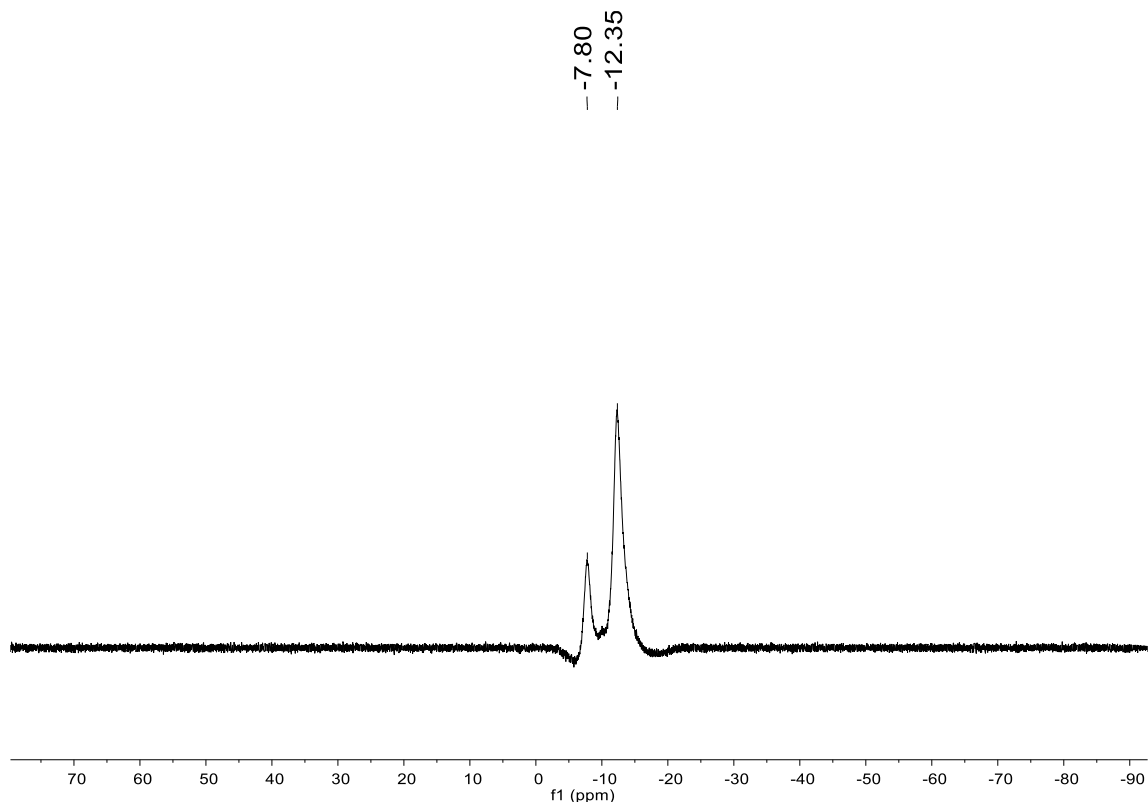
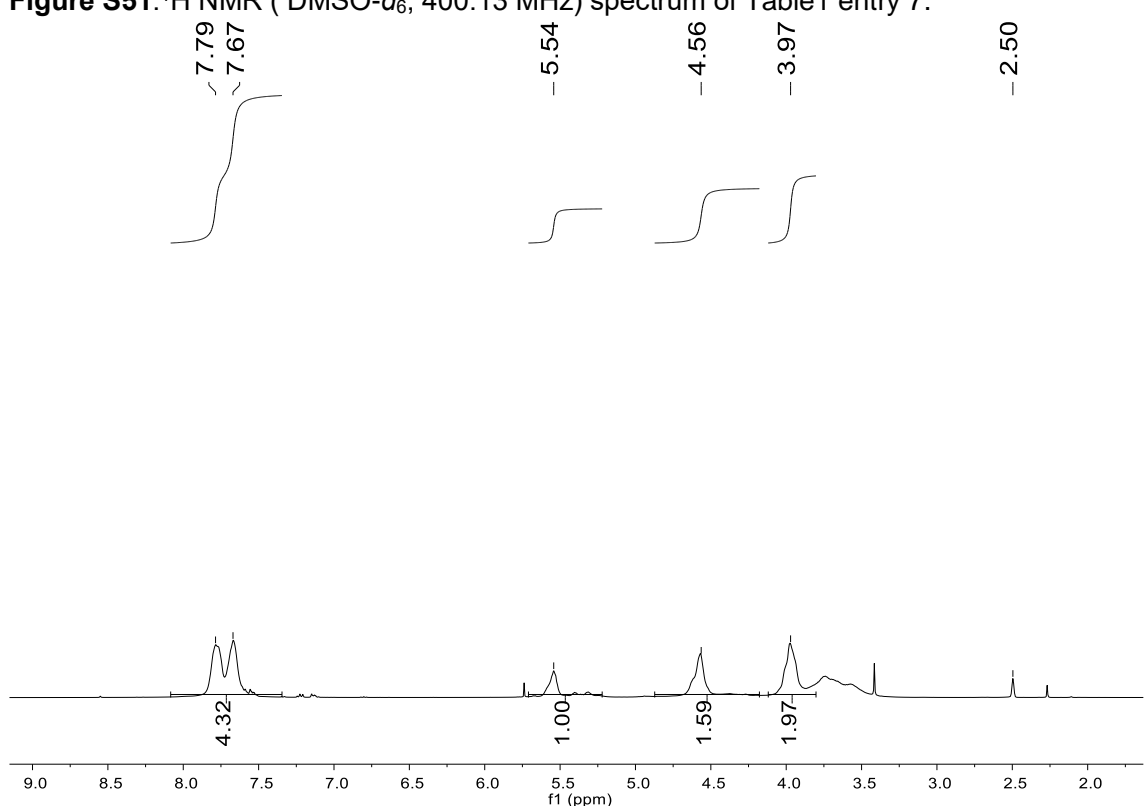
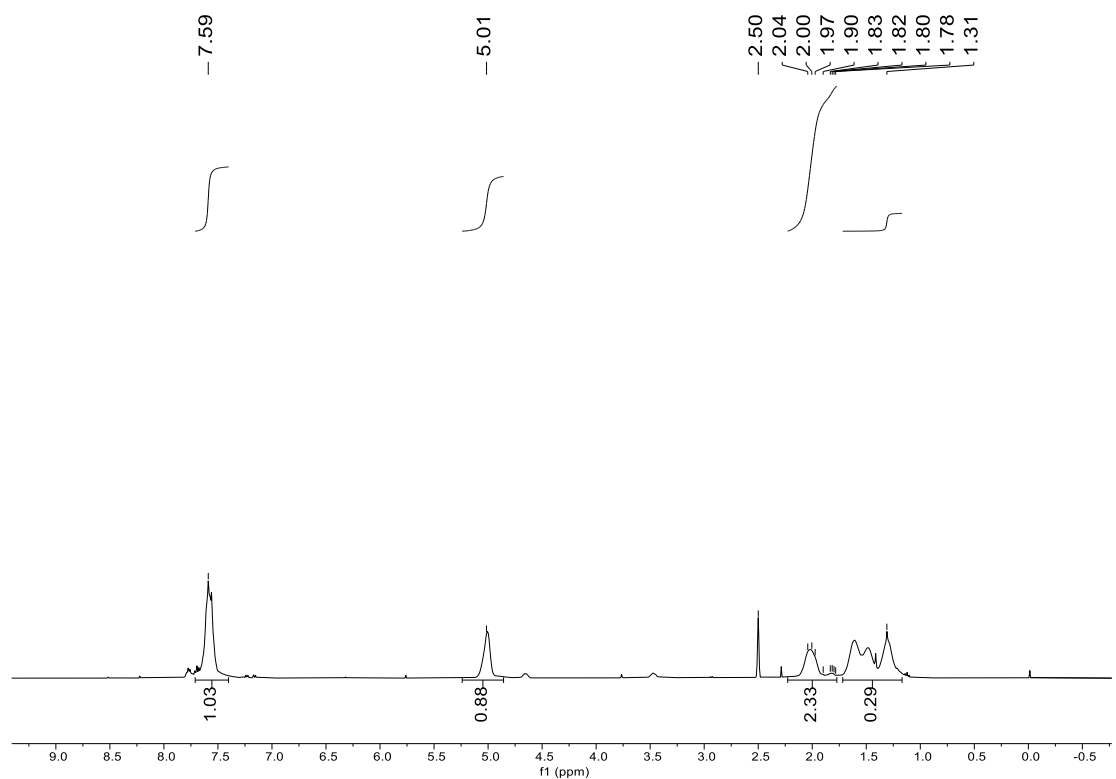


Figure S50. $^{11}\text{B}\{\text{H}\}$ NMR (CDCl_3 , 160.46 MHz) spectrum of compound **1d**.

(3) General Procedure for ROCOP

The polymerization was carried out using standard Schlenk techniques. A 25 mL reaction tubes was charged with the desired amounts of zinc catalysts, co-catalysts (PPNCl), phthalic anhydride, freshly distilled epoxides (2.55 mmol) and 5 mL toluene. The reaction mixture was heated and stirred for desired time, during which time an increase in viscosity was observed. The reaction was quenched by addition of a few drops of 1 M HCl aqueous solution. The polymer was isolated by methanol precipitation, filtering, and drying under vacuum at 50 °C for 6 h.

Following the optimization of the model ROCOP (catalyst **3b**, catalyst/co-catalyst ratio; 1:4, reaction time: 16 hours, temperature: 110 °C.), various co-monomers were explored to assess the scope for producing structurally diverse polyesters. (Table S1)



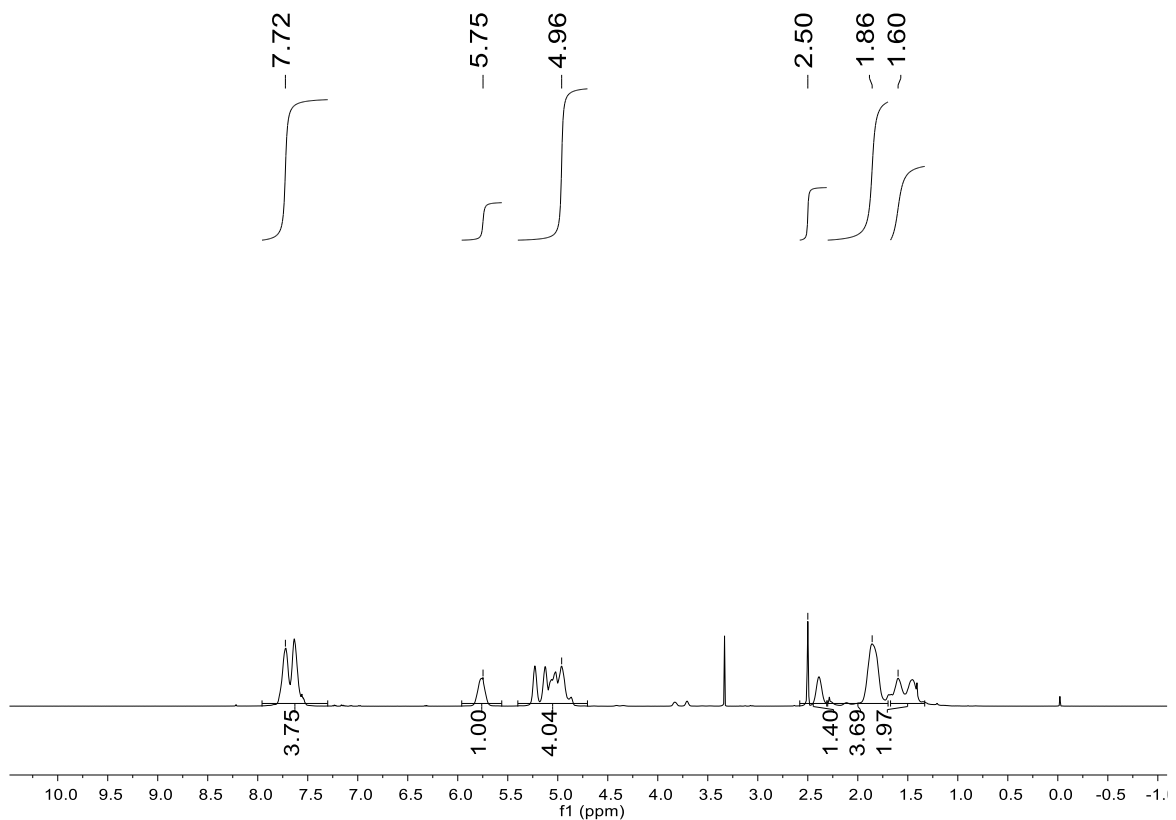


Figure S53. ¹H NMR (DMSO-*d*₆, 400.13 MHz) spectrum of Table S2 entry 2.

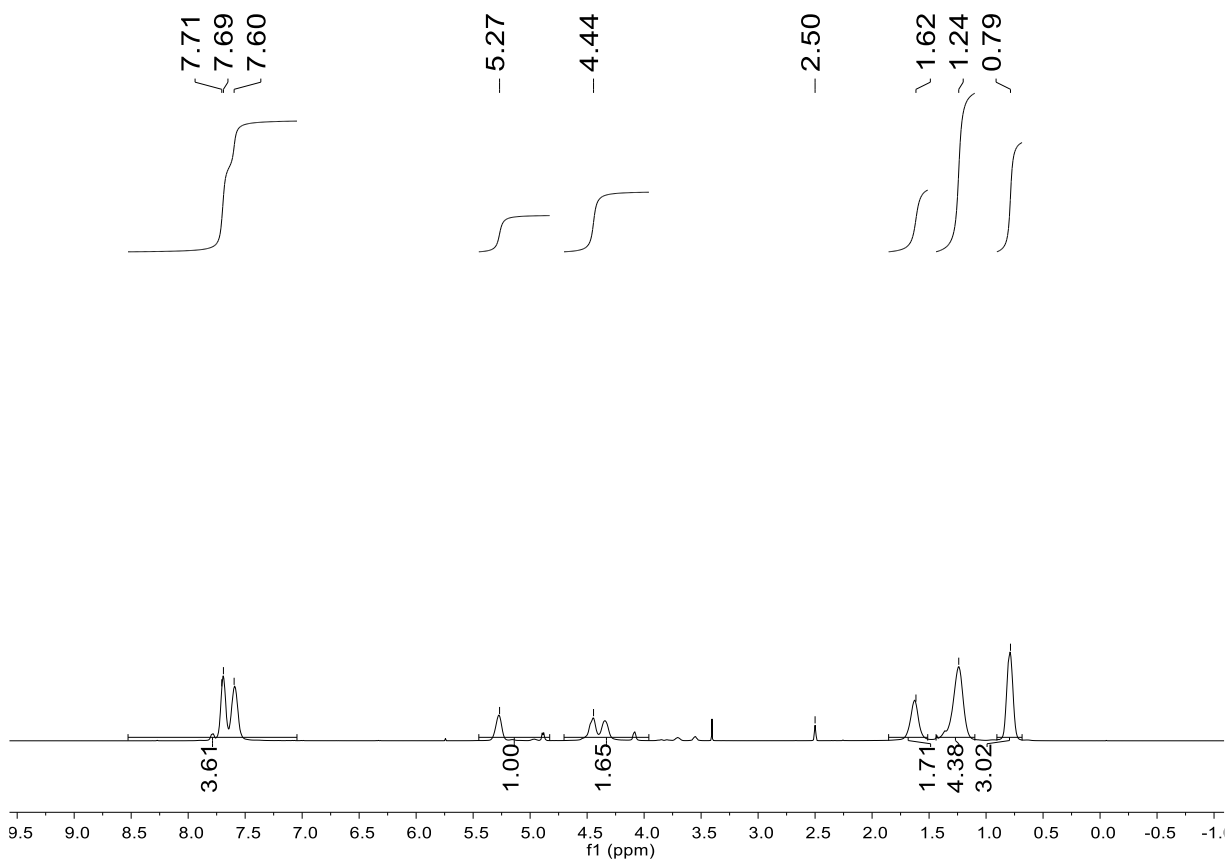
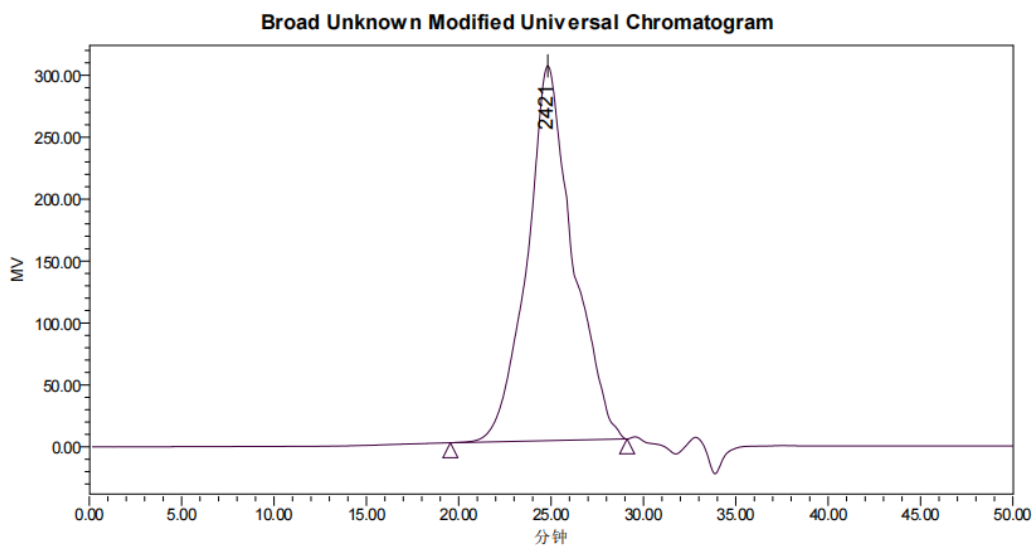


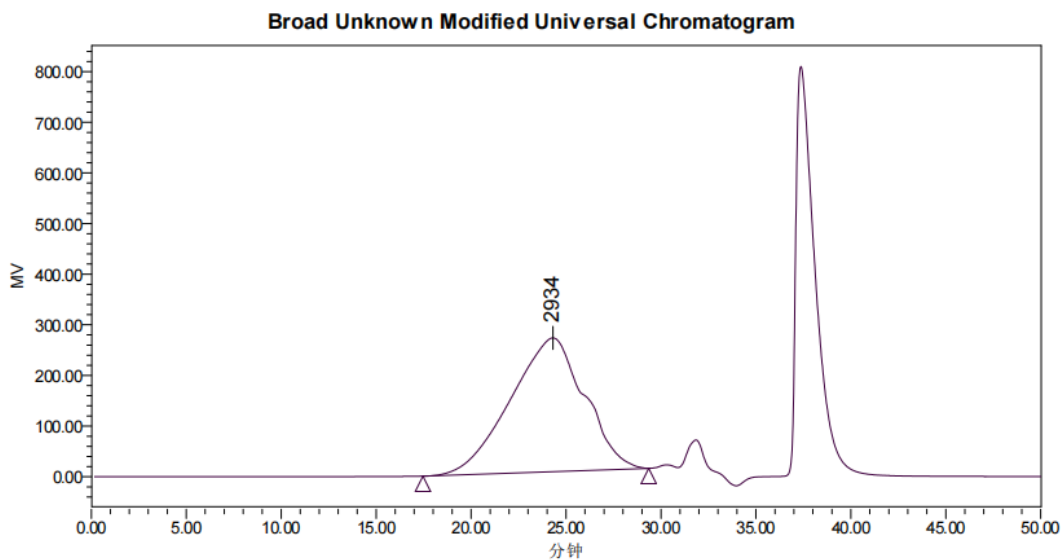
Figure S54. ¹H NMR (DMSO-*d*₆, 400.13 MHz) spectrum of Table S2 entry 3.

(4) GPC data of polymers



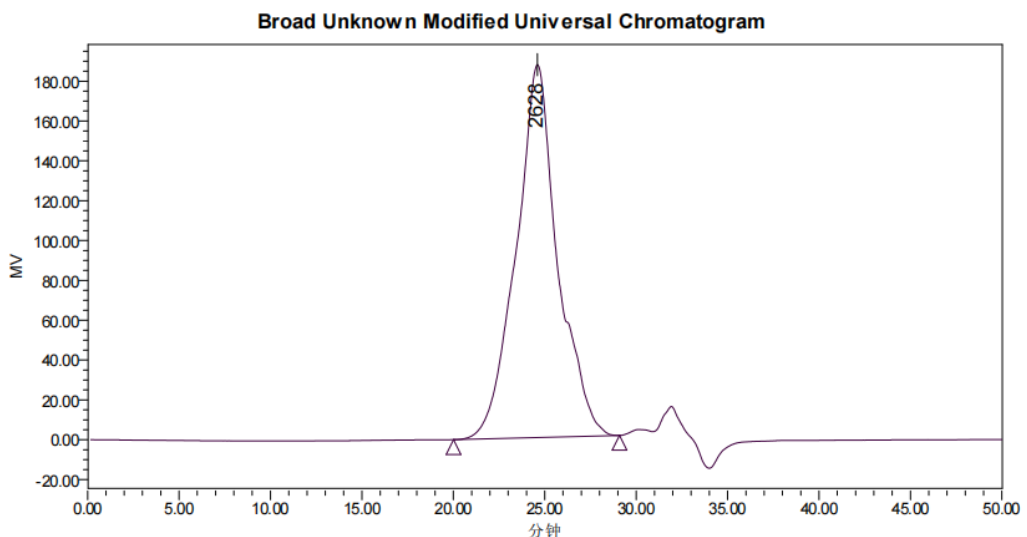
	Distribution Name	Mv (Daltons)	K (dl/g)	alpha	Intrinsic Viscosity (dl/g)	Mn (Daltons)	Mw (Daltons)	MP (Daltons)	Mz (Daltons)	Mz+1 (Daltons)	Polydispersity	Mz/Mw
1						1880	2571	2421	3411	4607	1.367156	1.326910

Figure S55. GPC data of Table1 entry 13.



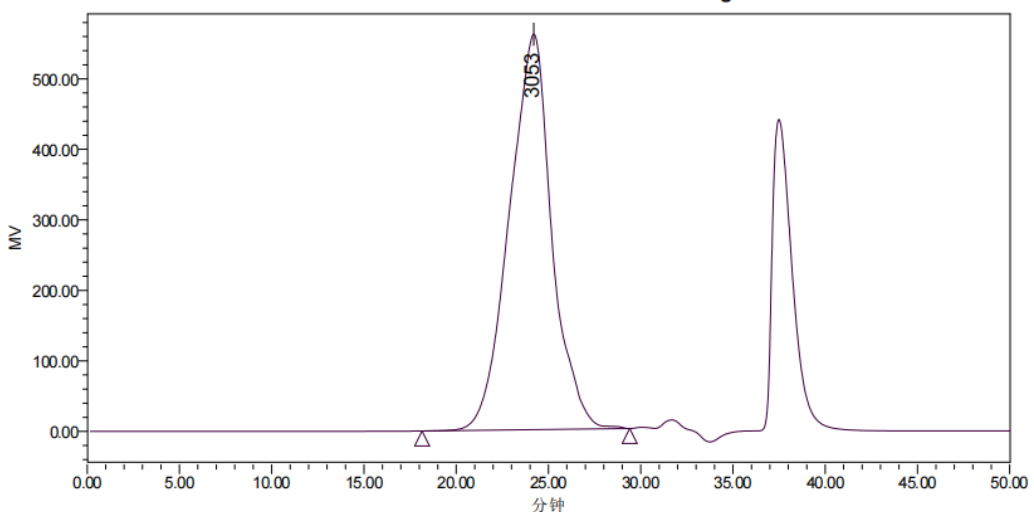
	Distribution Name	Mv (Daltons)	K (dl/g)	alpha	Intrinsic Viscosity (dl/g)	Mn (Daltons)	Mw (Daltons)	MP (Daltons)	Mz (Daltons)	Mz+1 (Daltons)	Polydispersity	Mz/Mw
1						2592	4861	2934	9243	15331	1.875380	1.901326

Figure S56. GPC data of Table S2 entry 1.



	Distribution Name	Mv (Daltons)	K (dl/g)	alpha	Intrinsic Viscosity (dl/g)	Mn (Daltons)	Mw (Daltons)	MP (Daltons)	Mz (Daltons)	Mz+1 (Daltons)	Polydispersity	Mz/Mw
1						2321	2988	2628	3830	4968	1.287178	1.281660

Figure S57. GPC data of Table S2 entry 2.
Broad Unknown Modified Universal Chromatogram



	Distribution Name	Mv (Daltons)	K (dl/g)	alpha	Intrinsic Viscosity (dl/g)	Mn (Daltons)	Mw (Daltons)	MP (Daltons)	Mz (Daltons)	Mz+1 (Daltons)	Polydispersity	Mz/Mw
1						2925	3765	3053	4865	6511	1.286992	1.292253

Figure S58. GPC data of Table S2 entry 3.

(5) X-ray crystallographic details

For X-ray structure analyses, the oil-coated crystals were mounted onto a loop, and the diffraction data were collected on a Bruker Smart Apex II or Bruker D8-Venture diffractometer with graphite-monochromated Mo K α ($\lambda = 0.71073 \text{ \AA}$) at the requested

temperature . An empirical (multi-scan) absorption correction was applied with the program SADABS.² The structures were solved by Olex2³ with the ShelXT⁴ solution program using the intrinsic phasing method and subsequently refined on F_2 with the ShelXL⁵ refinement package (SHELXL-2014) using full-matrix least-squares minimization techniques. If not noted otherwise, all non-hydrogen atoms were refined anisotropically, and hydrogen atoms were located at calculated positions or found in the ΔF map. Figures of the solid-state molecular structures were generated using XP as implemented in the SHELXTL program.

Molecular structures of **2a**, **3b** and **4a**, as well as the pertinent structure parameters, were given in Fig. S59-S61. Crystal data, data collection parameters, and the results of the analysis of these compounds are listed in Tables S1. Crystallographic data for the structures of compounds reported in this paper have been deposited with the Cambridge Crystallographic Data Center as supplementary publication numbers CCDC 2444573-2444575.

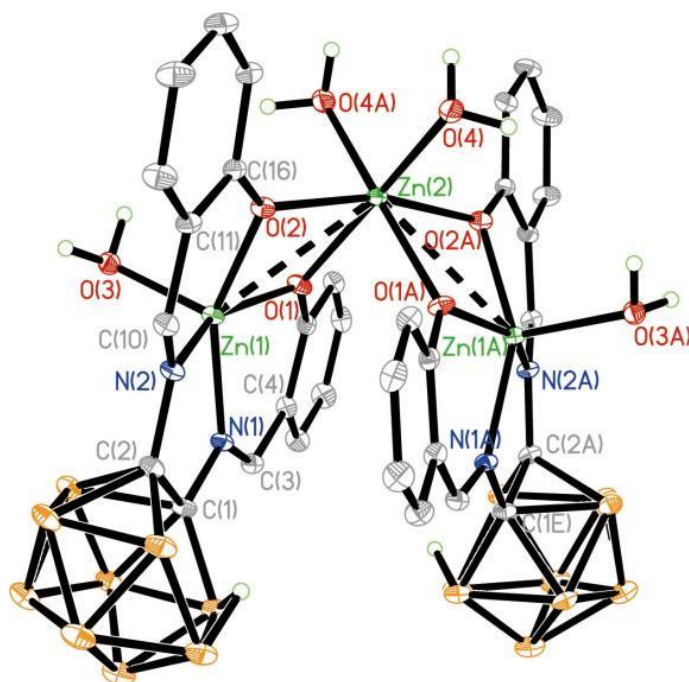


Figure S59. Molecular structure of **2a**. Molecular structure of **2a** (Some of the hydrogen atoms are omitted for clarity, ellipsoids set at the 30% probability level). Selected bond lengths (\AA) and angles($^\circ$): C(1)-C(2) 1.594(6), Zn(1)-Zn(2) 3.1277(7), Zn(1)-O(1) 1.993(3), Zn(1)-O(2) 1.981(3), Zn(1)-O(3) 2.046(3), Zn(1)-N(1) 2.042(3), Zn(1)-N(2) 2.044(3), Zn(2)-O(1) 2.103(3), Zn(2)-O(2) 2.123(3), Zn(2)-O(4) 2.048(3), N(1)-C(1) 1.446(5), N(1)-C(3) 1.280(5), N(2)-C(2) 1.436(5), N(2)-C(10) 1.284(5); O(1)-Zn(1)-O(3) 97.09(12), O(1)-Zn(1)-N(1) 89.98(12), O(1)-Zn(1)-N(2) 152.95(13), O(2)-Zn(1)-O(1) 81.70(11), O(2)-Zn(1)-O(3) 100.86(12), O(2)-Zn(1)-N(1) 150.72(13), O(2)-Zn(1)-N(2) 91.72(12), O(3)-Zn(1)-Zn(2) 111.59(8), N(1)-Zn(1)-Zn(2) 119.03(10), N(1)-Zn(1)-O(3) 108.03(13), N(1)-Zn(1)-N(2) 83.02(13), N(2)-Zn(1)-Zn(2) 121.86(10), N(2)-Zn(1)-O(3) 109.93(13), Zn(1A)-Zn(2)-Zn(1) 100.32(3), O(1A)-Zn(2)-Zn(1) 81.18(8), O(1) -Zn(2)-O(1A) 86.77(16), O(1A)-Zn(2)-O(2) 93.06(11),

O(1A)-Zn(2)-O(2A) 75.94(11), O(1)-Zn(2)-O(2) 75.94(11), O(1)-Zn(2)-O(2A) 93.06(11),
 O(2A)-Zn(2)-Zn(1) 127.84(8), O(2)-Zn(2)-O(2A) 165.01(15), O(4)-Zn(2)-Zn(1) 134.08(10),
 O(4)-Zn(2)-Zn(1A) 100.30(9), O(4A)-Zn(2)-O(1) 90.00(12), O(4)-Zn(2)-O(1) 172.77(13),
 O(4A)-Zn(2)-O(2) 92.42(12), O(4)-Zn(2)-O(2) 97.80(12), O(4)-Zn(2)-O(4A) 93.92(19), C(1)-N(1)-Zn(1)
 115.0(3), C(3)-N(1)-Zn(1) 124.4(3), C(3)-N(1)-C(1) 120.5(4), C(2)-N(2)-Zn(1) 114.8(3), C(10)-N(2)-Zn(1)
 123.8(3), C(10)-N(2)-C(2) 121.4(4), N(1)-C(1)-C(2) 112.4(3), N(2)-C(2)-C(1) 113.0(3)

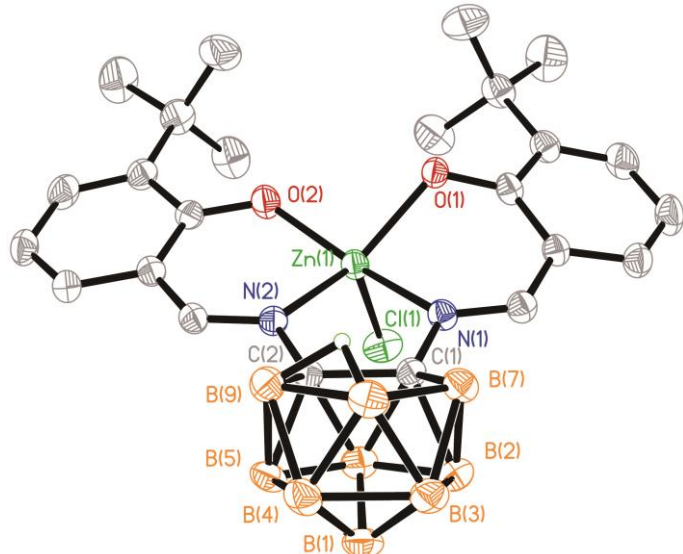


Figure S60. Molecular structure of **3a** (Some of the hydrogen atoms are omitted for clarity, ellipsoids set at the 30% probability level). Selected bond lengths (\AA) and angles($^{\circ}$): C(1)-C(2) 1.584(4), Zn(1)-Cl(1) 2.3454(13), Zn(1)-O(1) 2.027(2), Zn(1)-O(2) 1.955(2), Zn(1)-N(1) 2.133(3), Zn(1)-N(2) 2.107(2); O(1)-Zn(1)-Cl(1) 107.51(7), O(1)-Zn(1)-N(1) 82.54(9), O(1)-Zn(1)-N(2) 137.85(9), O(2)-Zn(1)-Cl(1) 103.43(8), O(2)-Zn(1)-O(1) 95.10(8), O(2)-Zn(1)-N(1) 157.74(10), O(2)-Zn(1)-N(2) 88.52(9), N(1)-Zn(1)-Cl(1) 98.35(8), N(2)-Zn(1)-Cl(1) 112.41(7), N(2)-Zn(1)-N(1) 78.91(10), C(1)-N(1)-Zn(1) 117.25(18), C(2)-N(2)-Zn(1) 117.97(18), C(3)-N(2)-Zn(1) 123.0(2).

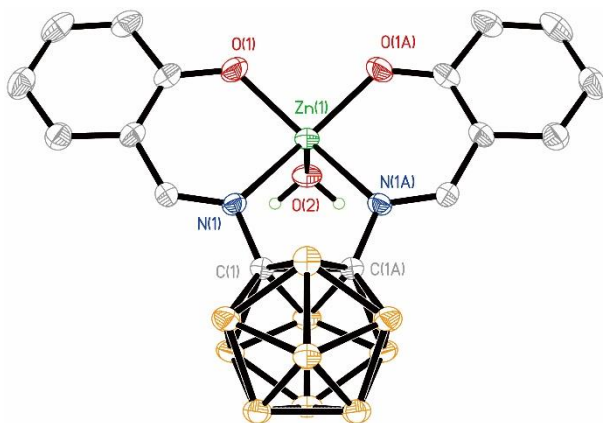


Figure S61. Molecular structure of **4a** (Some of the hydrogen atoms are omitted for clarity, ellipsoids set at the 30% probability level). Selected bond lengths (\AA) and angles($^{\circ}$): C1-C(1A) 1.667(5), Zn1-O1 1.973(2), Zn1-O2 2.012(3), Zn1-N1 2.124(2), N1-C1 1.421(3), N1-C2 1.291(3); O(1A)-Zn1-O1 92.87(13), O(1A)-Zn1-O2 102.20(9), O1-Zn1-O2 102.20(9), O1-Zn1-N1 87.59(9), O1-Zn1-N(1A) 153.88(10), O(1A)-Zn1-N1 153.88(10), O(1A)-Zn1-N(1A) 87.59(9), O2-Zn1-N(1A) 103.21(9), O2-Zn1-N1 103.21(9), N(1A)-Zn1-N1 80.87(12), C1-N1-Zn1 115.94(17), C2-N1-Zn1 125.00(19), C2-N1-C1 118.9(2), N1-C1-C11 112.49(14).

Table S1. Details of crystallographic data for **2a**, **3a** and **4a**

	2a	3b	4a
Empirical formula	C ₄₈ H ₈₄ B ₁₈ N ₄ O ₁₄ Zn ₃	C ₃₇ H ₆₉ B ₉ Cl ₄ N ₄ O ₂ Zn	C ₁₆ H ₂₂ B ₁₀ N ₂ O ₃ Zn
Formula weight	1331.88	906.42	463.82
Temperature (K)	106.55	296.15	173.00
Wavelength (Å)	0.71073	0.71073	0.71073
Crystal system	monoclinic	triclinic	orthorhombic
space group	C2/c	P-1	Pnma
a (Å)	31.280(3)	10.390(6)	8.8274(8)
b (Å)	13.2146(11)	12.226(7)	17.7768(12)
c (Å)	22.686(4)	22.240(13)	13.8438(12)
α (°)	90	103.925(12)	90
β (°)	128.651(2)	99.199(12)	90
γ (°)	90	97.975(12)	90
V (Å ³)	7323.3(14)	2660(3)	2172.4(3)
Z	4	2	4
D _{calcd} (g / cm ³)	1.208	1.132	1.418
μ (mm ⁻¹)	1.029	0.695	1.153
F(000)	2768.0	956.0	944.0
θ range (°)	3.334 ~ 56.664	3.492 ~ 61.01	5.474 ~ 58.23
Limiting indices	-41 ≤ h ≤ 33, -17 ≤ k ≤ 17, -28 ≤ l ≤ 30	-14 ≤ h ≤ 14, -17 ≤ k ≤ 16, -31 ≤ l ≤ 31	-12 ≤ h ≤ 12, -24 ≤ k ≤ 19, -16 ≤ l ≤ 18
Ref. collected/unique	29602/9077	34030/14512	12163/2981
R _{int}	0.0810	0.0744	0.0937
Data / restraints / parameters	9077/475/422	14512/524/550	2981/1/158
GOOF ^a	1.007	0.960	1.052
Final R indices [I > 2σ(I)] ^b	R ₁ = 0.0501, wR ₂ = 0.1088	R ₁ = 0.0642, wR ₂ = 0.1417	R ₁ = 0.0498, wR ₂ = 0.1107
R indices (all data)	R ₁ = 0.0974, wR ₂ = 0.1264	R ₁ = 0.1441, wR ₂ = 0.1737	R ₁ = 0.0741, wR ₂ = 0.1251
Δρ _{max, min} (e/Å ³)	0.62/-0.56	0.43/-0.55	0.37/-0.56

^a Goodness-of-fit on F^2 ^b $R_1 = ||F_O| - |F_C||/|F_O|$, $wR_2 = [\sum w(F_O^2 - F_C^2)^2 / \sum w(F_O^2)]^{1/2}$

(6) References

- 1 (a) Y. Kang, B. Wang, R. Nan, Y. Li, Z. Zhu and X.-Q. Xiao, *Inorg. Chem.*, 2022, **61**, 8806-8814; (b) R. Pang, J. Li, Z. Cui, C. Zheng, Z. Li, W. Chen, F. Qi, L. Su and X. Q. Xiao, *Dalton Trans.*, 2019, **48**, 7242-7248; (c) J. Li, R. Pang, Z. Li, G. Lai, X. Q. Xiao and T. Müller, *Angew. Chem. Int. Ed.*, 2019, **58**, 1397-1401.
- 2 (a) G. M. Sheldrick, *Journal*, 1996; (b) G. Sheldrick, *University of Göttingen, Göttingen, Germany*, 1994, **90**.
- 3 O. V. Dolomanov, L. J. Bourhis, R. J. Gildea, J. A. K. Howard and H. Puschmann, *J. Appl. Crystallogr.*, 2009, **42**, 339-341.
- 4 Bruker, *Bruker Analytical X-ray Instruments Inc., Madison, Wisconsin, USA*, 2014.
- 5 G. M. Sheldrick, *Acta Crystallogr.*, 2015, **C71**, 3-8.